Biochimie 186 (2021) 130–146

Contents lists available at ScienceDirect

Biochimie

journal homepage: www.elsevier.com/locate/biochi

Neuroprotective effect of 6-hydroxy-2,2,4-trimethyl-1,2-dihydroquinoline mediated via regulation of antioxidant system and inhibition of inflammation and apoptosis in a rat model of cerebral ischemia/reperfusion

E.D. Kryl'skii [a, *], E.E. Chupandina [b], T.N. Popova [a], Kh.S. Shikhaliev [c], V.O. Mittova [d], S.S. Popov [e], A.N. Verevkin [a], A.A. Filin [b]

[a] Department of Medical Biochemistry and Microbiology, Voronezh State University, Russia
[b] Department of Pathological Anatomy, Voronezh State Medical University named after N.N. Burdenko, Russia
[c] Department of Organic Chemistry, Voronezh State University, Russia
[d] Department of Biochemistry, Voronezh State Medical University named after N.N. Burdenko, Russia
[e] Department of Organization of Pharmaceutical Business, Clinical Pharmacy and Pharmacognosy, Voronezh State Medical University named after N.N. Burdenko, Russia

ARTICLE INFO

Article history:
Received 5 March 2021
Received in revised form
21 April 2021
Accepted 29 April 2021
Available online 5 May 2021

Keywords:
Cerebral ischemia/reperfusion
Oxidative stress
Dihydroquinoline derivatives
Inflammation
Apoptosis
Antioxidants

ABSTRACT

The aim of the study was the assessment of the neuroprotective potential of 6-hydroxy-2,2,4-trimethyl-1,2-dihydroquinoline (DHQ) and its effect on inflammation, apoptosis, and transcriptional regulation of the antioxidant system in cerebral ischemia/reperfusion (CIR) in rats.

The CIR rat model was constructed using the bilateral common carotid artery occlusion followed by reoxygenation. DHQ was administered at a dose of 50 mg/kg for three days. Histological staining was performed using hematoxylin and eosin. The level of S100B protein, 8-hydroxy-2-deoxyguanosine, and 8-isoprostane was assessed using an enzyme immunoassay. The intensity of apoptosis was assessed based on the activity of caspases and DNA fragmentation. The activity of enzymes was measured spectrophotometrically, the level of gene transcripts was assessed by real-time PCR.

DHQ reduced the histopathological changes and normalized levels of S100B, lactate, pyruvate, and HIF-1 mRNA in the CIR rat model. In addition, DHQ decreased the oxidative stress markers in animals with a pathology. The tested compound also inhibited inflammation by decreasing the activity of myeloperoxidase, expression of interleukins and *Nfkb2*. DHQ-treated rats with CIR showed decreased caspase activity, DNA fragmentation, and AIF expression. DHQ changed activity of antioxidant enzymes to the control values, decreased the expression of *Cat*, *Gsr*, and *Nfe2l2*, which was overexpressed in CIR, and activated the expression of *Sod1*, *Gpx1*, *Gsta2*, and *Foxo1*.

DHQ showed a neuroprotective effect on CIR in rats. The neuroprotective effect involve mechanisms such as the inhibition of oxidative stress, leading to a reduction in the inflammatory response and apoptosis and the modulation of the antioxidant defense components.

1. Introduction

Strokes are the second leading cause of death worldwide, killing about 6.7 million people every year [1]. Strokes occur due to impaired cerebral circulation, leading to a decrease in oxygen levels, the inhibition of oxidative phosphorylation in mitochondria, and energy deficiency in the ischemic area. Reoxygenation from reperfusion following ischemia can lead to additional tissue damage [2]. The excessive generation of reactive oxygen species (ROS) in the mitochondrial electron transport chain is considered to be the main mechanism of neuronal cell death during reperfusion [3,4].

Cell protection against reactive molecules is provided by antioxidant enzymes [5]. The main transcriptional regulator of antioxidant protection in mammals is the NF-E2-related factor 2 (Nrf2)-Kelch-like ECH-associated protein 1 (Keap1) system. Under oxidative stress

* Corresponding author. 394018, Universitetskaya sq. 1, Voronezh, Russia.
E-mail address: krylskiy@bio.vsu.ru (E.D. Kryl'skii).

https://doi.org/10.1016/j.biochi.2021.04.010
0300-9084/

Abbreviations

ROS	reactive oxygen species
Nrf2	NF-E2-related factor 2
Keap1	Kelch-like ECH-associated protein 1
AREs	antioxidant responsive elements
FOXO1	forkhead box protein O1
NF-κB	nuclear factor kappa B
DHQ	6-hydroxy-2,2,4-trimethyl-1,2-dihydroquinoline
CIR	cerebral ischemia/reperfusion
PASS	Prediction of Activity Spectra for Substances
LD50	lethal dose 50
8OHDG	8-hydroxy-2-deoxyguanosine
BChL	biochemiluminescence
POM	protein oxidative modification
2,4-DNPH	2,4-dinitrophenylhydrazine
TCA	trichloroacetic acid
DC	diene conjugates
MPO	myeloperoxidase
TMB	3,3′,5,5′-tetramethylbenzidine
SOD	superoxide dismutase
NBT	nitro blue tetrazolium
GP	glutathione peroxidase
GR	glutathione reductase
GT	glutathione-S-transferase
G6PDH	glucose-6-phosphate dehydrogenase
NADP-IDH	NADP-isocitrate dehydrogenase
GSH	reduced glutathione
AIF	apoptosis inducing factor
HIF-1	hypoxia inducing factor
DAMP	damage associated molecular patterns
PPP	pentose phosphate pathway
AH	aconitate hydratase

conditions, the Nrf2-Keap1 complex is dissociated, the released Nrf2 translocates to the nucleus, heterodimerizes with one of the small Maf proteins and recognize AREs (antioxidant responsive elements), that are enhancer sequences present in the regulatory regions of Nrf2 target genes [6]. Another regulatory protein playing an important role in cell survival under oxidative stress is the transcription factor forkhead box protein O1 (FOXO1) [7,8].

Inflammation plays a key role in the pathogenesis of ischemia/reperfusion. After ischemic injury, brain endothelium and astrocytes secrete large amounts of chemokines and cytokines. These agents stimulate the expression of adhesion molecules on the endothelium, leading to the leukocyte adhesion and the degradation of endothelium tight junction proteins and the degradation of the extracellular matrix. The damaged blood-brain barrier promotes both the penetration of peripheral inflammatory cells into the brain and an increase in the secretion of mediators, leading to permanent damage to the barrier [9]. The NF-κB (nuclear factor kappa B) transcriptional activation pathway is considered the main mediator of inflammatory responses in nervous and vascular tissues. In a steady-state condition heterodimeric NF-κB p65/p50 complexes are bound with the inhibitory factor IκBα in the cytoplasm. The IκB kinase is rapidly phosphorylated and activated after cerebral ischemia/reperfusion, causing phosphorylation and degradation of IκBα. Thus, the p65/p50 dimer is released and transported into the nucleus, where it promoting the expression of proinflammatory cytokines [10].

Cerebral ischemia and reperfusion can activate various cell death pathways such as necrosis, apoptosis, or autophagy. Among these, apoptosis is considered a key event in ischemic brain damage. The activation of classical apoptosis occurs in two main ways. One of these is the ligand-mediated pathway, which is initiated by the activation of cell surface death receptors such as Fas, and leading to the activation of caspase-8 or caspase-10. The other is the mitochondrial apoptosis pathway, which originates from the mitochondrial release of cytochrome C and subsequent activation of caspase-9. Both pathways lead to signaling cascades that converge in the activation of effector caspase-3, which ultimately leads to apoptosis [11].

The analysis of compounds possessing simultaneously high antioxidant and anti-inflammatory potential is expedient, since oxidative stress plays a central role in the pathogenesis of ischemia/reperfusion. These compounds include antioxidant ethoxyquin (6-ethoxy-2,2,4-trimethyl-1,2-dihydroquinoline) [12]. Our *in silico* analysis revealed more promising compounds for drug precursors with the higher antioxidant activity among the dihydroquinoline derivatives. One of the selected compounds, 6-hydroxy-2,2,4-trimethyl-1,2-dihydroquinoline (DHQ), was synthesized and tested by us as a neuroprotective agent.

In this study, we assessed the neuroprotective and antioxidant potential of DHQ, and examined its effect on the inflammation, apoptosis, and transcriptional regulation of the antioxidant system in rats with cerebral ischemia/reperfusion (CIR).

2. Materials and methods

2.1. DHQ synthesis

The synthesis of DHQ was carried out according to a well-known method by dealkylation of 6-ethoxy-2,2,4-trimethyl-1,2-dihydroquinoline (ethoxyquin) when exposed to hydrobromic acid (Appendix 1) [13]. The structure of the synthesized compounds was confirmed by NMR, IR spectroscopy, and gas chromatography-mass spectrometry.

2.2. Prediction of biological activity spectra and toxicity of DHQ

The biological activity of dihydroquinoline derivatives was assessed using the Prediction of Activity Spectra for Substances (PASS) biological activity analysis program [14–17]. The prediction of the toxicity of the compound was carried out by *in silico* analysis using the PROTOX program [18,19]. This program predicts the lethal dose (LD50) of the tested compound. According to the analysis, all substances are classified into six Globally Harmonized System of Classification and Labeling of Chemicals categories, depending on the toxicity of the compound: Category I: LD50 $\leq$ 5 mg/kg; Category II: 5 < LD50 $\leq$ 50 mg/kg; Category III: 50 < LD50 $\leq$ 300 mg/kg; Category IV: 300 < LD50 $\leq$ 2000 mg/kg; Category V: 2000 < LD50 $\leq$ 5000 mg/kg; Category VI: LD50 > 5000 mg/kg.

2.3. Animals and CIR model

Male Wistar rats 4–6 months old and weighing 200–250 g were used in this study. Rats were kept under conditions of a 12 h light/dark cycle. The animals were provided with food and water *ad libitum*. The study's protocols were approved by the Institutional Animal Care and Use Committee of Voronezh State University (Voronezh, Russia) and correspond to EU Directive 2010/63/EU for animal experiments. For the induction of CIR, anesthetized rats were placed in a supine position on an operating table. The body

temperature of each rat was maintained with an incandescent lamp. After shaving, a middle incision was made to expose both common carotid arteries. The dissection was performed between the sternocleidomastoid and sternohyoid muscles parallel to the trachea. The incision area was regularly treated with novocaine. Each common carotid artery was dissected from the adventitia membrane and carefully detached from the vagus nerve. For the induction of ischemia, both common carotid arteries were clamped with a silk thread for 30 min, followed by reperfusion [20]. The restoration of blood flow was monitored visually.

2.4. Experimental design

Groups (n = 10 per group) were formed by the random assignment of rats as follows: group 1 (control) of sham-operated animals received 0.5 ml of physiological solution intraperitoneally; group 2 (CIR) of rats with CIR; group 3 (CIR + DHQ) of rats intraperitoneally administrated with DHQ at a dose of 50 mg/kg dissolved in 0.5 ml of saline, 3 h after induction of CIR with an interval of 24 h; group 4 (control + DHQ) of sham operated rats received DHQ at a dose of 50 mg/kg according to the above scheme. The dosage of the tested compound was chosen based on the therapeutic doses of the nootropic piracetam and the experimental animals were dosed according to their body weight. On the fourth day from the beginning of the experiment, rats were sacrificed, brain and blood were extracted and immediately used for biochemical analysis. In each experiment, the brain and blood of two experimental animals were examined. Each investigated indicator in the samples was analyzed in triplicate. The scheme of the experiment is shown in Fig. 1.

2.5. Assessment of the brain metabolic state of laboratory animals

Determination of the lactate content in the brains of laboratory animals was performed using the diagnostic kit “Lactat-01" (Olvex Diagnosticum, Russia). Pyruvate concentration was detected using the “Pyruvate UV-Abris +" kit (NPF Abris +, Russia).

2.6. Determination of S100B, 8-isoprostane and 8-hydroxy-2-deoxyguanosine

The S100B protein level was determined using an S100 Calcium Binding Protein B ELISA Kit (Cloud-Clone Corp., USA). The 8-isoprostane concentration was assessed using a Rat 8-isoprostane ELISA Kit (Puda Scientific, China). The level of 8-hydroxy-2-deoxyguanosine (8OHDG) was measured using an 8-hydroxy-2-deoxyguanosine ELISA kit (Abcam, UK). The plates were washed with a Stat Fax 2600 washer (Awareness Technology, USA); the results were detected by a Stat Fax 4300 Chromate ELISA photometer (Awareness Technology, USA).

2.7. Histological staining

Hematoxylin-eosin staining of brain was assessed in three rats from each group. Rats were anesthetized, each brain was rapidly removed and immersed in 10% formalin for 2 h, then washed three times using the PBS. After being dehydrated and embedded with paraffin, the brain tissues were cut into 6-μm-thick coronal sections by rotary microtome HM-325 (Thermo Fisher Scientific, USA) for the hematoxylin-eosin staining. The sections were counterstained with hematoxylin in nucleuses and differentiated by eosin in cytoplasm. High magnification images were captured using an AxioLab A1 light microscope (Zeiss, Germany). A minimum of five fields for each slide were evaluated. Identification of the dead cells was done by morphological criteria by the blebbing in the plasma membrane and shrunken cytoplasm, surrounded by perineuronal vacuoles, neuron size alteration, and triangular shape of the cells.

2.8. Assessment of the oxidative stress intensity

The oxidative stress intensity and the total antioxidant activity in the sample were measured by biochemiluminescence (BChL) induced by hydrogen peroxide with iron sulfate [21]. The BChL kinetic curve was recorded for 30 s using a BChL-07 biochemiluminometer (Medozons, Russia), and the following parameters were determined: the light sum of chemiluminescence (S), maximum intensity (Imax), tangent of the BChL kinetic curve slope ($tg\alpha_2$). The reaction medium contained 0.4 ml of 0.02 mM potassium phosphate buffer (pH 7.5), 0.4 ml of 0.01 mM $FeSO_4$ and 0.2 ml of a 2% hydrogen peroxide solution introduced immediately before the measurement. The test material was added in a volume of 0.1 ml before the introduction of hydrogen peroxide.

The method of Reznick et al. [22] with minor modifications was used for the analysis of the protein oxidative modification (POM). The method is based on the ability of the carbonyl amino acid residues react with 2,4-dinitrophenylhydrazine (2,4-DNPH) with the formation of 2,4-dinitrophenylhydrazones. Briefly, the sample was diluted with 100 mM phosphate buffer (pH 7.4), then 10 mM 2,4-DNPH dissolved in 2.5 M HCl was added, the mixture was incubated for 1 h and then 20% trichloroacetic acid (TCA) was added. After cooling, the samples were centrifuged at 3000 g, the protein precipitate was washed with 10% TCA and a mixture of ethanol and ethyl acetate (1:1), and then dissolved in 2 ml of 8 M urea. The optical density of the experimental sample was measured at 370 nm relative to the control sample treated with 2.5 M hydrochloric acid. The molar extinction coefficient $\xi = 22.000\ cm^{-1} \times M^{-1}$ was used for the calculation of the content of carbonyl amino acid groups in proteins (nM).

For the analysis of the diene conjugates (DC) concentration, heptane and isopropanol were added to the test sample, mixed and precipitated by centrifugation at 3000*g*. The heptane phase of the supernatant was diluted with ethanol and analyzed spectrophotometrically at 233 nm [23].

2.9. Enzyme activities assays

Aconitate hydratase (AH) activity was estimated in a 50 mM Tris-HCl buffer (pH 7.8) containing 4 mM sodium citrate (“PanReac”, Spain). Myeloperoxidase (MPO) activity was measured using 3,3′,5,5′-tetramethylbenzidine (TMB, Sigma). A 10 μl sample was mixed with 80 μl of 0.75 mM H_2O_2 (Sigma) and 110 μl of a TMB solution (2.9 mM TMB in 14.5% DMSO and 150 mM potassium-phosphate buffer pH 5.4) and the plate was incubated for 5 min at 37 °C. The reaction was stopped by adding 50 μl of 2 M H_2SO_4 and the absorption was measured at 450 nm [24]. Superoxide dismutase (SOD) activity was measured by the indirect method developed by Nishikimi et al. based on the reduction of nitro blue tetrazolium (NBT) [25]. In this assay, SOD competes for the superoxide radicals generated in the presence of PMS and NADH reducing the reduction of NBT. The reaction mixture consisted of 0.33 mM EDTA, a 0.1 M phosphate buffer (pH 7.8), 0.8 mM NADH, 0.41 mM NBT, and 0.01 mM PMS. The absorbance of the formed blue formazan was measured at 540 nm. Catalase activity was assessed according to the spectrophotometric assay developed by Goth [26]. The reaction mixture contained 0.08% hydrogen peroxide in 0.1 M Tris-HCl buffer (pH 7.4) as a substrate. The decomposition of hydrogen peroxide by catalase was terminated by adding 4.5% ammonium molybdate. The intensity of the formed yellow complex was measured at 410 nm. Glutathione peroxidase (GP) activity was assayed according to Paglia and Valentina [27]. Hydrogen peroxide (0.37 mM) and GSH (0.85 mM) were used as substrates and coupled oxidation of NADPH (0.12 mM) by GR (1 U/ml)

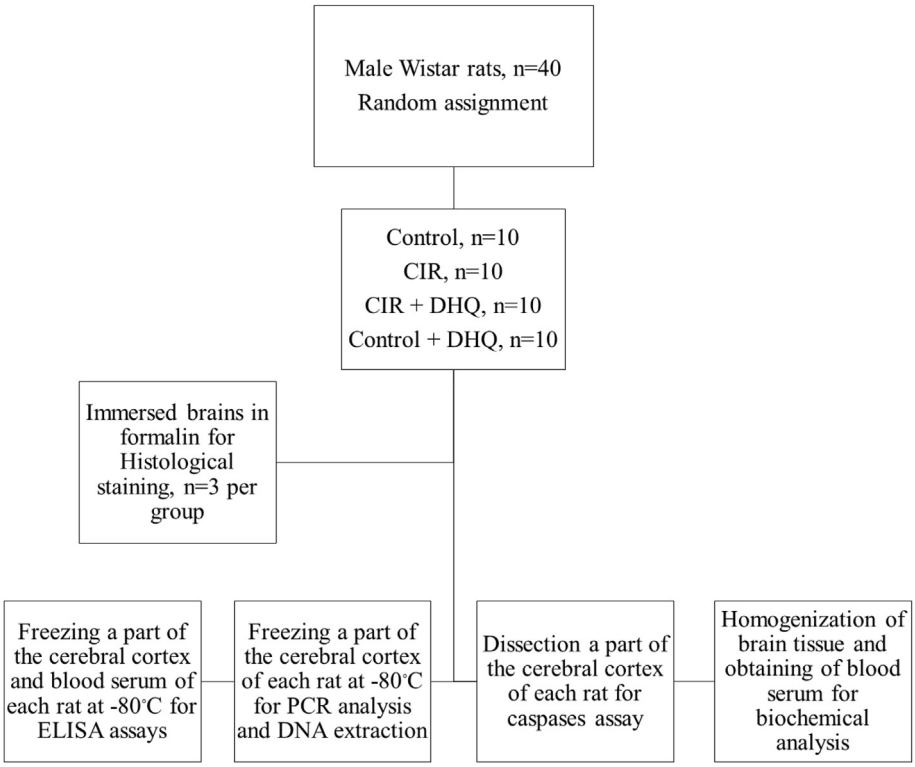

Fig. 1. The scheme of the experiment.

was determined at a wavelength of 340 nm. Glutathione reductase (GR) activity was evaluated by measuring the oxidation of NADPH (0.16 mM) using oxidized glutathione as a substrate [28]. The reaction mixture contained a 50 mM potassium phosphate buffer (pH 7.4), 0.8 mM oxidized glutathione, 0.16 mM NADPH, and 1 mM EDTA. Glutathione-S-transferase (GT) activity was assessed by the method of Warholm et al. using GSH and 1-chloro-2,4-dinitrobenzene acid as substrates [29]. The media for the determination of glucose-6-phosphate dehydrogenase (G6PDH) activity consisted of a 50 mM Tris-HCl buffer (pH 7.8) containing 3.2 mM glucose-6-phosphate, 0.25 mM NADP, and 1.0 mM $MgCl_2$. The activity of NADP-isocitrate dehydrogenase (NADP-IDH) was measured in a media consisting of 50 mM Tris-HCl buffer (pH 7.8), 1.5 mM isocitrate, 2 mM MnCl2, and 0.4 mM NADP. The enzymatic activity was evaluated by the change in optical density at 340 nm using a Hitachi U1900 spectrophotometer (Japan). The protein content was determined by Lowry's method.

2.10. Determination of the content of non-enzymatic antioxidants

The concentration of reduced glutathione (GSH) was determined by the reaction with 5.5-ditio-bis-(2-nitrobenzoic) acid ("Sigma Aldrich", USA), in which a thionitrophenyl anion having a yellow color and a maximum absorption at 412 nm is formed in equimolar amounts [30]. The sample was mixed with a 0.1 M phosphate buffer at pH 7.4.20% trichloroacetic acid was added and then thoroughly mixed. Then the mixture was left in the refrigerator for 15–20 min. Then, the samples were centrifuged at 3000 g. The phosphate buffer was added into the supernatant obtained by centrifugation. Ellman's reagent and 96% ethanol were added to the experimental and control samples, respectively. The content of the tubes was thoroughly mixed and the optical density of the experimental and control samples was analyzed at λ 412 nm against the phosphate buffer.

The concentration of citrate was evaluated according to the Natelson method [31]. The experimental sample was mixed with 17% TCA, centrifuged at 4000 g, after 50% H_2SO_4, 1 M potassium bromide, and saturated potassium permanganate solution were added to the supernatant. The resulting pentabromoacetate was extracted with petroleum ether. The ether extract was then mixed with 2% thiourea in a borate buffer. After phase separation, the lower layer was analyzed at 430 nm using a Hitachi U-1900 spectrophotometer.

The concentration of α-tocopherol was determined using the method based on photometry of the chromogenic complex compound Fe^{2+} and o-phenanthroline [32]. Ethanol and hexane were added to the test sample, centrifuged at 3000 g, after the hexane layer was taken and the hexane was evaporated in a water bath. Benzene and ferric chloride were added to the dry residue. After 5 min, 0.05% o-phenanthroline was added, then after 2 min the optical density was measured at 510 nm.

2.11. Determination of the intensity of apoptotic processes

The enzyme activities of caspase-8 and caspase-3 were measured using colorimetric assay kits purchased from BioVision (Milpitas, California, USA). The assay kits detected caspase activation by the spectrophotometric determination of p-nitroaniline produced via hydrolysis of acetyl-Ile-Glu-Thr-Asp p-nitroaniline and acetyl-Asp-Glu-Val-Asp p-nitroaniline by caspase-8 and caspase-3, respectively. The para-nitroaniline produced in the reaction was determined at 405 nm. The caspase activity was expressed in picomoles of the product formed per 1 min, per 1 mg protein.

Isolation of total DNA was performed using the K-Sorb kit (Syntol, Russia) in accordance with the manufacturer's instructions. DNA samples were been normalized using the elution buffer to 50 ng/μl in the total volume of 100 μl. DNA fragmentation was detected by agarose gel electrophoresis of the samples using a Tris-acetate buffer.

2.12. RNA isolation, reverse transcription, and quantitative PCR

Total RNA was isolated using the ExtractRNA reagent (Eurogen,

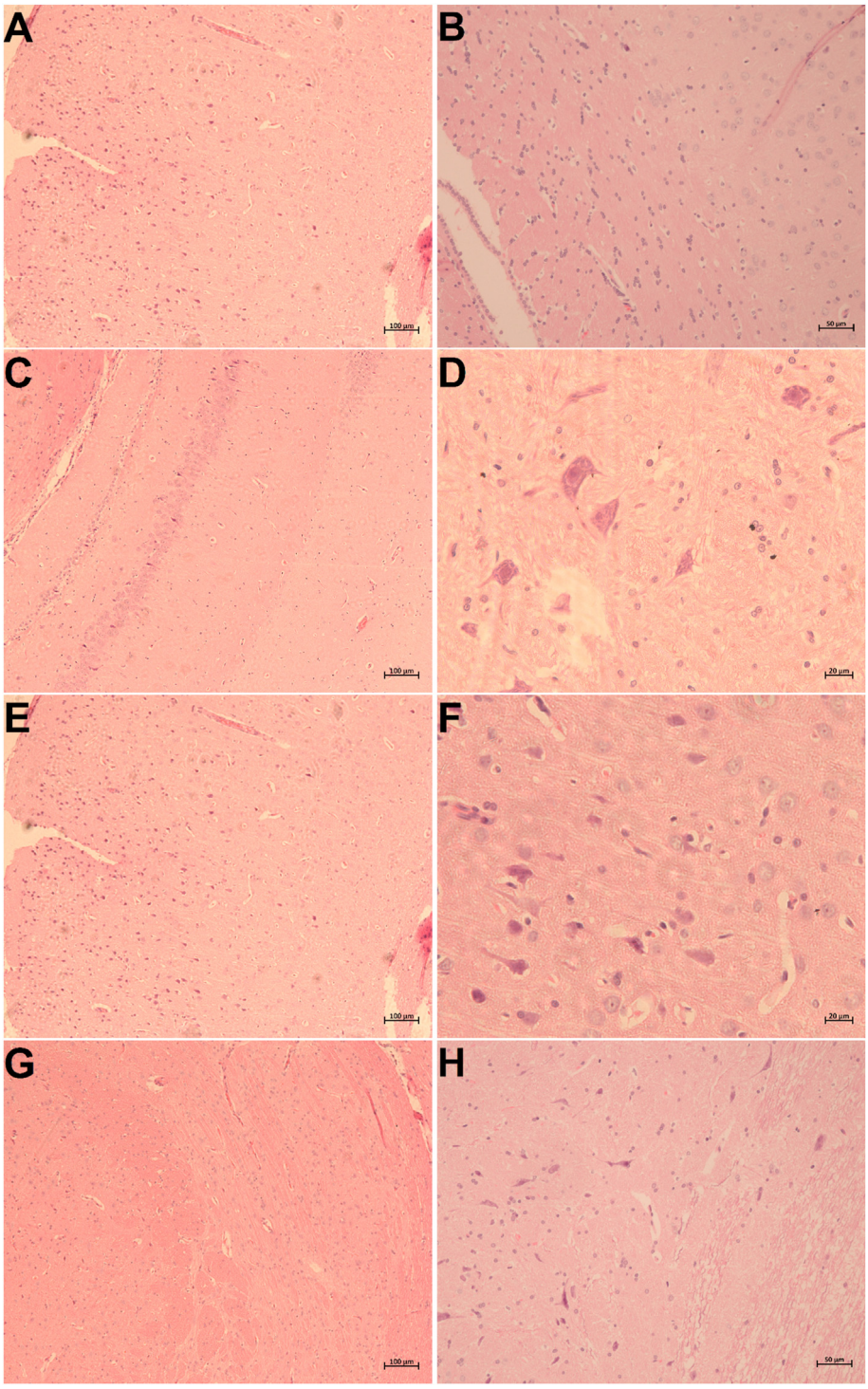

Fig. 2. Hematoxylin and eosin staining of the cerebral cortex tissues of rats. Neuronal damage was absent in the Control group (A, ×100 magnification; B, ×200 magnification), as well as in sham-operated animals receiving DHQ (G, ×100 magnification; H, ×200 magnification). CIR modeling caused the development of pathological changes in neurons (C, ×100 magnification; D, ×400 magnification), while the administration of DHQ at a dose of 50 mg/kg under ischemia/reperfusion conditions reduced the pathological changes (E, ×100 magnification; F, ×400 magnification).

Russia). The quality of RNA isolation was monitored using agarose gel electrophoresis. Reverse transcription was performed in two replicates using the MMLV RT kit (Eurogen, Russia) in accordance with the instructions. The amount of mRNA of each gene was normalized to the level of *Gapdh* and *Actβ* mRNAs used as housekeeping genes (Appendix 2). Real-time PCR was performed using qPCRmix-HS SYBR (Eurogen, Russia) with an ANK-32 device (Synthol, Russia). The analysis of the results was carried out using the $2^{-\Delta\Delta Ct}$ method. The specificity of the reaction was evaluated based on the melting curves.

2.13. Statistical analysis

Multiple groups were analyzed using a one-way ANOVA with Tukey's post hoc test, $p < 0.05$ was considered to be statistically significant. Statistical analysis was performed using the IBM SPSS

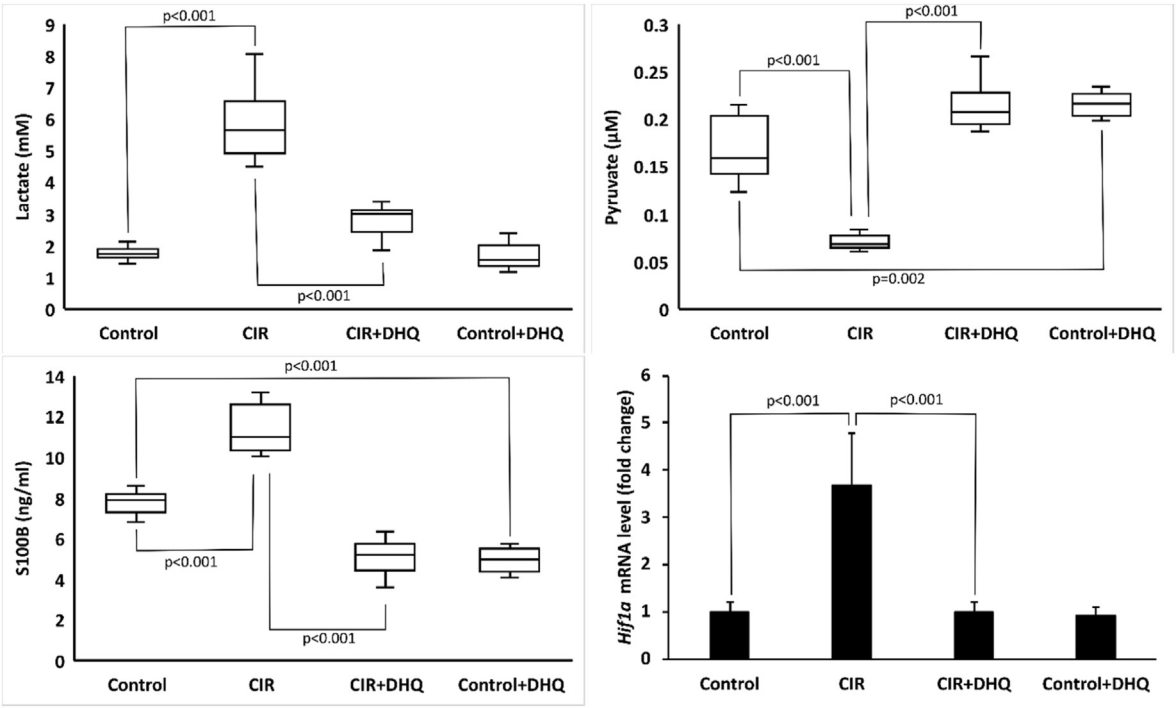

Fig. 3. The effect of DHQ on the markers of cerebral ischemia in rats. The development of CIR in rats was accompanied by an increase in the concentration of lactate in the brain and a decrease in the level of pyruvate, as well as the accumulation of *Hif1a* gene transcripts. The level of S100B in the serum increased in animals with the pathology. The administration of DHQ to rats with CIR changed these parameters towards the control values. Data in bars are presented as mean ± SD.

Statistics 25 software. All quantitative data were presented as the mean ± standard deviation (SD).

3. Results

3.1. Bioactivity and toxicity prediction of DHQ

The database of compounds of the Department of Organic Chemistry of Voronezh State University [33] was used for the virtual screening. A wide range of nitrogen-, oxygen-, and sulfur-containing heterocyclic compounds are presented in the database. The compounds are small drug-like molecules. The biological activity spectra of hydroquinoline derivatives were predicted using the computer program PASS (prediction of activity spectra for substances). Appendix 3 represents the results of the prediction of main types of biological activities of DHQ and the most promising candidates. The predicted biological activity of the compounds was compared to that of piracetam. DHQ, which has the highest antioxidant and protective potential, was selected for research.

In silico analysis of toxicity showed that DHQ is of class 4 toxicity with a predicted LD50 of 1450 mg/kg. Amino oxidase A (Avg Pharmacophore Fit 34.97%) and progesterone receptor (Avg Similarity Known Ligands 76.7%) are predicted among the targets of toxic action.

3.2. Effect of DHQ on histopathological changes in the CIR rat model

For morphological analysis, sections of the brain stained with hematoxylin and eosin were used (Fig. 2). As a result of the studies carried out on animals with CIR, a sharp decrease in the blood supply of the vessels of the microcirculation was found. The number of functioning capillaries was significantly reduced. There was a pronounced pericellular and perivascular edema, a large number of dystrophically altered neurons with a predominance of karyolysis. In places, hypertrophy and hyperchromicity of the nucleolus ectoped to the nuclear membrane and perinuclear hyperchromatosis were visualized. Some neurons had a honeycomb-like cytoplasm, some neurons were totally dark-colored, had narrower, elongated neurosome. Some neurons had central tinctorial acidophilia. In addition, dystonia of the vascular walls, thickening and coarsening of argyrophilic fibers, perivascular edema, and rarely small perivascular hemorrhages were observed.

In turn, DHQ administration at a dose of 50 mg/kg significantly attenuated the histopathological changes in the brain cortex. Therefore, DHQ may reduce brain damage caused by cerebral ischemia and reperfusion.

3.3. Aerobic metabolism and the level of markers of cerebral ischemia

For the assessment of the state of the aerobic metabolism in the brains of animals we evaluated lactate and pyruvate levels in the brain tissues of rats with CIR and subsequently injected with DHQ. The accumulation of lactate, the end product of anaerobic glycolysis, as well as a decrease in the pyruvate concentration, was found in brain tissues of rats with pathology. The administration of DHQ to animals with CIR changed the levels of these metabolites towards the control values ($p < 0.05$, Fig. 3). In addition, the level of S100B in the serum increased in rats with CIR. The development of CIR was also associated with the induction of HIF-1 (*Hif1a* gene) expression. The treatments with DHQ led to a decrease ($p < 0.05$) in these parameters (Fig. 3).

3.4. DHQ reduces oxidative stress in animals with CIR

We have previously shown that the modeling of CIR in rats led to an increase in BChL parameters, DC content, POM level, and AH inhibition [34]. In addition, the development of the pathology was associated with an increase in such markers of oxidative stress as 8-

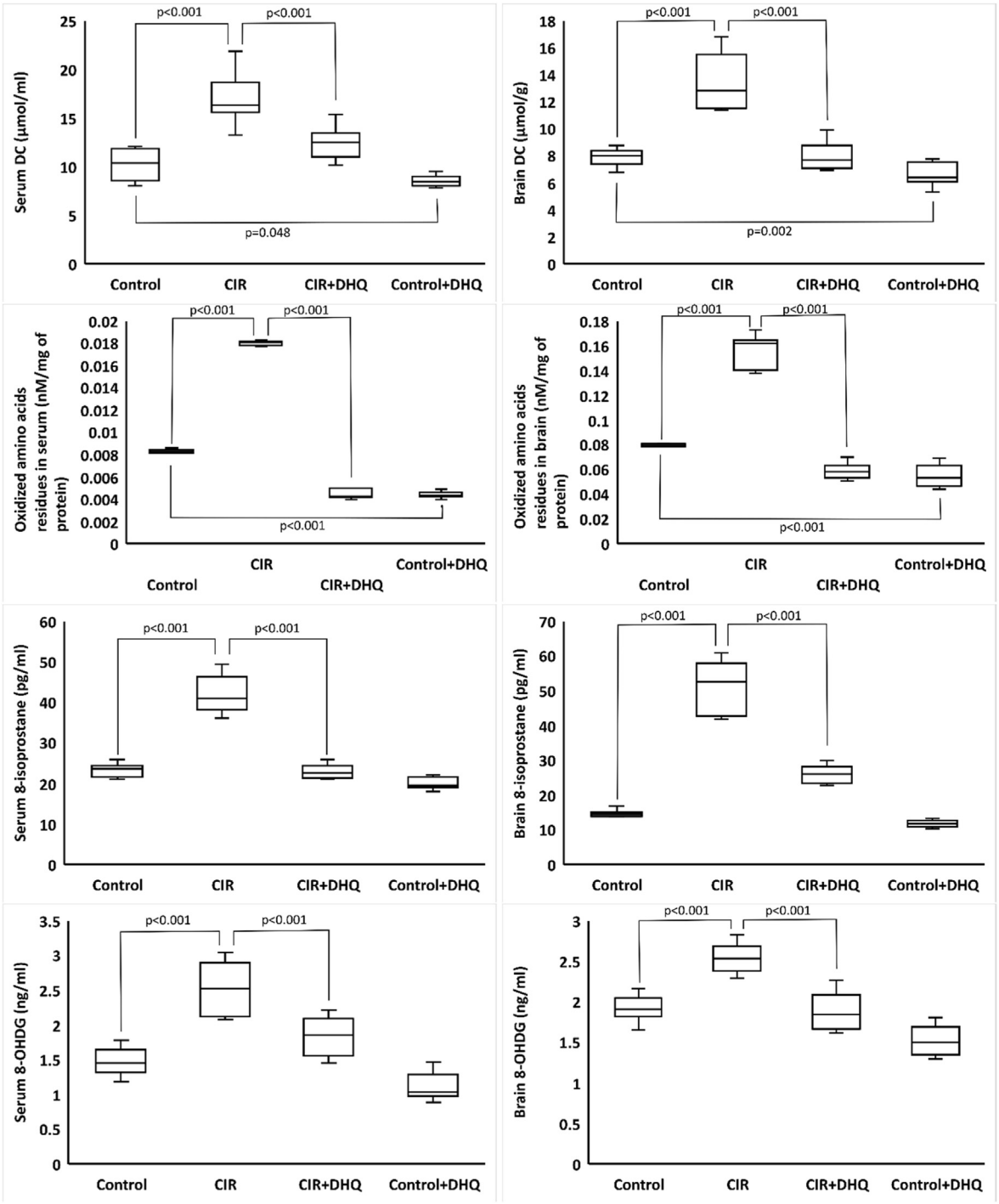

Fig. 4. Effects of DHQ on oxidative stress markers in CIR. Administration of DHQ to animals with CIR significantly reduced DC content, POM level, concentration of 8-isoprostane and 8-OHDG in the brain and blood serum.

isoprostane and 8-OHDG. The administration of DHQ to rats with CIR led to a significant ($p < 0.05$) decrease in the markers of oxidative stress and restoration of AH activity (Fig. 4, Table 1).

3.5. Anti-inflammatory effect of DHQ in CIR rats

CIR is associated with the activation of an inflammatory response. As our studies shown, the administration of DHQ to animals with CIR led to a significant ($p < 0.05$) decrease in the expression of proinflammatory cytokines, such as TNF-α, IL-1β, IL-6 (encoded by the *Tnf*, *Il1b*, and *Il6* genes), and the transcription factor NF-κB (*Nfkb2* gene). The level of cyclooxygenase-2 transcripts (*Ptgs* gene) in the CIR + DHQ group changed insignificantly. Among other things, DHQ reduced ($p < 0.05$) MPO activity in tissues of animals with CIR (Fig. 5).

3.6. DHQ administration to CIR animals reduces apoptosis in brain

In previous studies, we have demonstrated that CIR in animals is associated with the increased activity of caspase-3, caspase-8, and DNA fragmentation [34]. In addition, in the present work, it was shown that the level of apoptosis inducing factor (AIF) transcripts

Table 1
Effects of DHQ on BChL parameters and AH activity in CIR animals. Administration of DHQ to animals with CIR led to a decrease in Imax and S, showing the intensity of free radical-induced oxidation, as well as tgα_2, characterizing the degree of antioxidant system mobilization. In addition, DHQ promoted the restoration of AH activity inhibited under CIR conditions. Data are presented as mean ± SD. * - $p < 0.05$ compared to Control; ** - $p < 0.05$ compared to CIR.

Groups	Blood serum				Brain			
	Control	CIR	CIR + DHQ	Control + DHQ	Control	CIR	CIR + DHQ	Control + DHQ
I_{max}, mV	1.72 ± 0.45	3.68 ± 0.61*	2.23 ± 0.51**	1.52 ± 0.23*	6.12 ± 1.46	13.61 ± 3.04*	5.83 ± 1.06**	5.29 ± 1.19*
S, mV*s	11.66 ± 2.45	26.85 ± 6.8*	13.11 ± 2.66**	9.48 ± 1.84*	33.10 ± 8.99	58.99 ± 15.77*	38.36 ± 8.82**	29.77 ± 6.28*
tgα_2	1.93 ± 0.45	4.75 ± 1.14*	1.87 ± 0.41**	1.81 ± 0.33*	1.09 ± 0.19	2.63 ± 0.67*	1.02 ± 0.34**	0.90 ± 0.19*
AH, U/ml serum, U/g brain tissue	1.12 ± 0.35	0.521 ± 0.11*	1.047 ± 0.42**	1.15 ± 0.51	2.18 ± 0.72	0.831 ± 0.25*	1.683 ± 0.51**	2.22 ± 0.75
AH, U/mg protein	0.065 ± 0.021	0.013 ± 0.004*	0.052 ± 0.015**	0.068 ± 0.020	0.368 ± 0.115	0.156 ± 0.051*	0.205 ± 0.071**	0.375 ± 0.112

(gene *Aifm1*) increased in the brains of animals with the pathology. The present study showed, that the administration of DHQ to CIR rats led to a significant ($p < 0.05$) decrease in the activity of caspase-3 and caspase-8 and *Aifm1* expression (Fig. 6).

3.7. DHQ decreases the mobilization of antioxidant enzymes in CIR

As we have shown in previous studies, the modeling of CIR in rats led to the activation of SOD, catalase, GP, GR, and GT, which was of a compensatory effect [35,36]. The administration of DHQ to animals with the pathology led to a decrease in the severity of oxidative stress and load on antioxidant enzymes, which contributed to a decrease ($p < 0.05$) in their activity (Appendix 4). Enzyme activity, expressed as E/mg protein, changed in a similar way (Appendix 5).

3.8. DHQ provides a normalization of non-enzymatic antioxidant concentrations in the tissues of CIR rats

CIR in rats was associated with an increase in the serum and brain levels of GSH and citrate, as well as the depletion of the α-tocopherol pool. The administration of DHQ to animals at the same time led to a significant ($p < 0.05$) decrease in the concentration of GSH and citrate, as well as the restoration of the α-tocopherol level in tissues (Fig. 7).

3.9. Effects of DHQ on the transcriptional regulation of antioxidant defense in CIR

As we have shown earlier, one of the most important mechanisms in the activation of antioxidant defense enzymes in CIR was the induction of their expression at the transcriptional level [34]. In particular, there was an increase in the transcript levels of SOD, catalase, GP, GR, and GT, and factors Nrf2 and Foxo1 (genes *Sod1*, *Cat*, *Gpx1*, *Gsr*, *Gsta2*, *Nfe2l2*, *Foxo1*, respectively). DHQ had a multidirectional effect on the expression of these genes. Thus, the analyzed compound led to a decrease ($p < 0.05$) in the expression of *Cat*, *Gsr*, and *Nfe2l2*, while the expression of *Sod1*, *Gpx1*, *Gsta2*, and *Foxo1* was increased in CIR + DHQ rats ($p < 0.05$; Fig. 8).

4. Discussion

In the course of this study, we analyzed the neuroprotective mechanisms of the DHQ effect and evaluated its regulatory effect on the antioxidant defense system in CIR rats. Our results demonstrated that the tested dihydroquinoline derivative reduced oxidative stress and modulated the functioning of the antioxidant defense system, contributing to the inhibition of inflammation and apoptosis, improvement of aerobic metabolism, and reducing histopathological changes in the cerebral cortex.

As is known, ischemia leads to the inhibition of aerobic metabolism and the formation of lactic acidosis [37]. In our studies, lactate accumulation and depletion of the pyruvate pool in the brain were shown in CIR rats. The level of these changes significantly decreased after the administration of DHQ. The main regulator of the metabolism, sensitive to the oxygen level, is the hypoxia inducing factor (HIF-1), which, as our data confirmed, is induced under ischemic conditions. During hypoxia, the HIF-1α protein undergoes rapid stabilization, leading to its nuclear translocation, binding with the aryl hydrocarbon receptor nuclear translocator, also designated as hypoxia-inducible factor (HIF)-1β with the formation of the HIF-1 transcription factor complex. Mature HIF-1 modulates the expression of more than 200 target genes and mediates the formation of hypoxia tolerance and a neuroprotective effect [38]. At the same time, HIF-1 activates the expression of vascular endothelial growth factor and matrix metalloproteinases, which have been shown to be involved in the disruption of the blood-brain barrier [39]. In addition, there is evidence that HIF-1, in addition to its neuroprotective effect, interacts with the p53 protein and causes delayed neuronal death caused by ischemia [40]. The administration of DHQ led to a decrease in the HIF-1α expression, which could be a consequence of the DHQ neuroprotective activity and the normalization of energy metabolism. The positive effect of DHQ was also confirmed by a change in the concentration of S100B in the serum, which is the biomarker of brain damage. With physiological concentrations, S100B acts as a neurotrophic factor, but an increase in its concentration may lead to the opposite effect. In addition, there is evidence of a positive correlation between the S100B level and neuron-specific enolase, a marker of brain neuronal loss [41]. Histopathological findings confirmed the neuroprotective effect of DHQ. The administration of DHQ significantly reduced the damage of neurons caused by CIR, which was associated with the leveling of morphological changes in neurons and an increase in cell survival.

Oxidative stress is the leading cause of tissue damage in CIR. Oxidative stress is characterized by the overproduction of ROS, causing mutations in mitochondrial DNA, damaging the mitochondrial respiratory chain, altering membrane permeability, affecting Ca^{2+} homeostasis and mitochondrial defense systems. Commonly, ROS are generated endogenously from molecular oxygen by cellular oxidases, mono- and dioxygenases of the mitochondrial electron chain transport system or peroxidases, and are involved in damage to nerve cells after ischemia/reperfusion [42,43]. Oxidative stress can activate the NF-κB signaling pathway to synthesize of pro-inflammatory mediators such as nitric oxide, TNF-α, IL-6, promoting inflammation in neurons, and matrix metalloproteinase-9, causing the destruction of the extracellular matrix and tight junction proteins with subsequent damage to the blood-brain barrier [44]. As our results demonstrated, in addition to an increase in oxidative stress markers, such as DC, POM, 8-OHDG, 8-isoprostane, and BChL parameters, inhibition of the AH activity, which is a sensitive target of ROS in CIR rats was also observed [45]. DHQ significantly reduced oxidative stress in rats with the pathology, probably due its antioxidant activity. Thus, a high reducing ability for this compound was predicted by *in silico* analysis ($p = 0.888$). Protective and antioxidant properties are also known

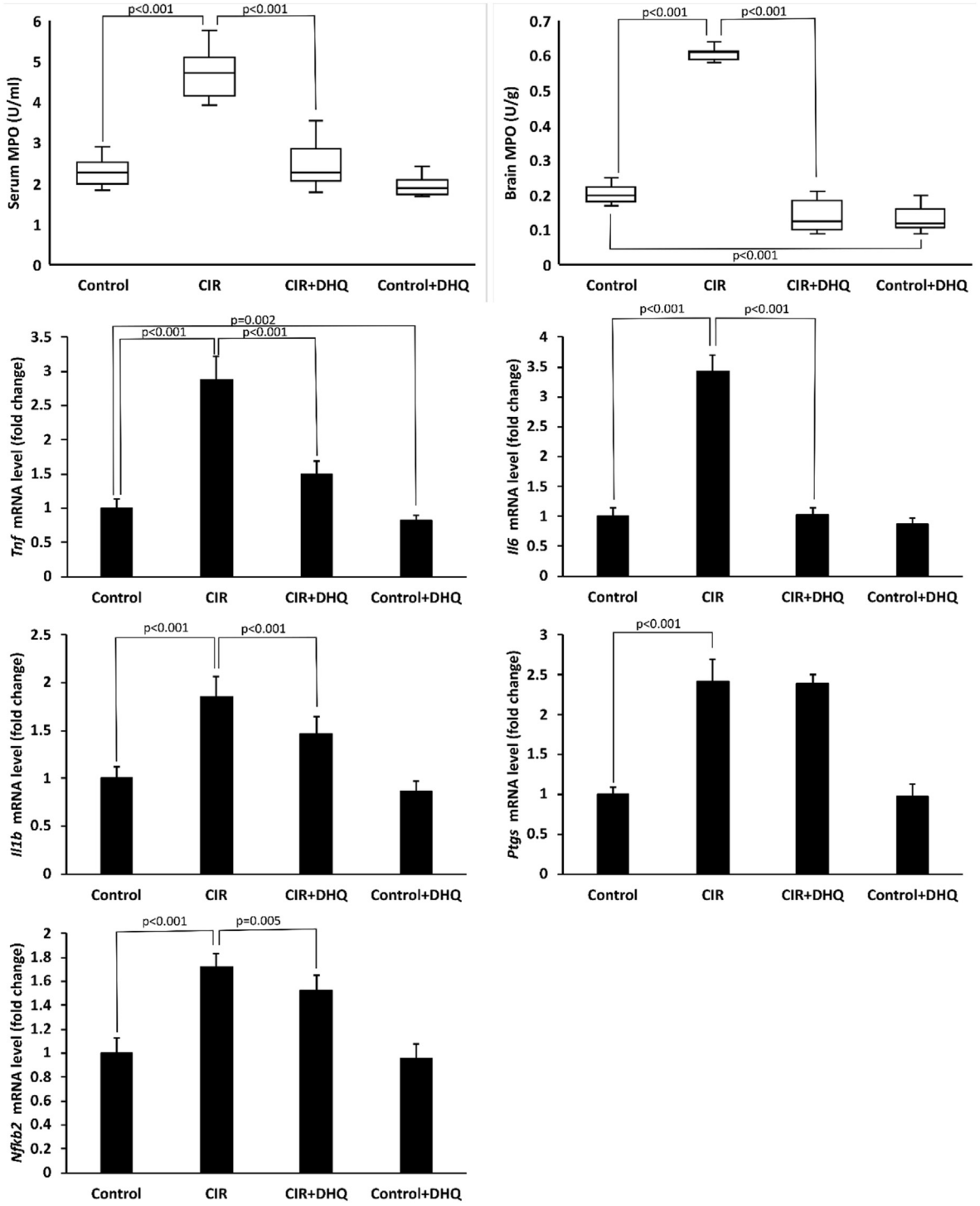

Fig. 5. The effect of DHQ on the inflammatory response in animals with CIR. The level of gene transcripts, represented in the form of a heat map, demonstrating that the administration of DHQ to animals with CIR led to a decrease in the expression of the proinflammatory cytokines TNF-α, IL-1β, IL-6, and factor NF-κB. In addition, exposure to DHQ reduced MPO activity in the serum and brain of CIR animals. Bars in histograms are presented as mean ± SD.

for other dihydroquinoline derivatives. Previously, the neuroprotective properties of a compound belonging to quinoline 1,2-dihydro derivatives - ethoxyquine [46] were established. It is also known that 8-hydroxyquinoline derivatives have the ability to reduce the level of β-amyloid, act as scavengers of free radicals, and chelates copper ions [47].

Oxidative stress can activate inflammation, another key mechanism for nerve tissue damage during ischemia/reperfusion. The immune response is triggered by the damage associated molecular patterns (DAMP) released from damaged cells. DAMPs are subsequently elicited by immune cells with appropriate receptors recognizing molecules, mediating the activation of intracellular signaling pathways. Within minutes after brain damage, microglia are activated, undergo morphological changes and secrete cytokines, which contributes to damage to the parenchyma and cerebral vessels. Blood-brain barrier impairment occurs immediately

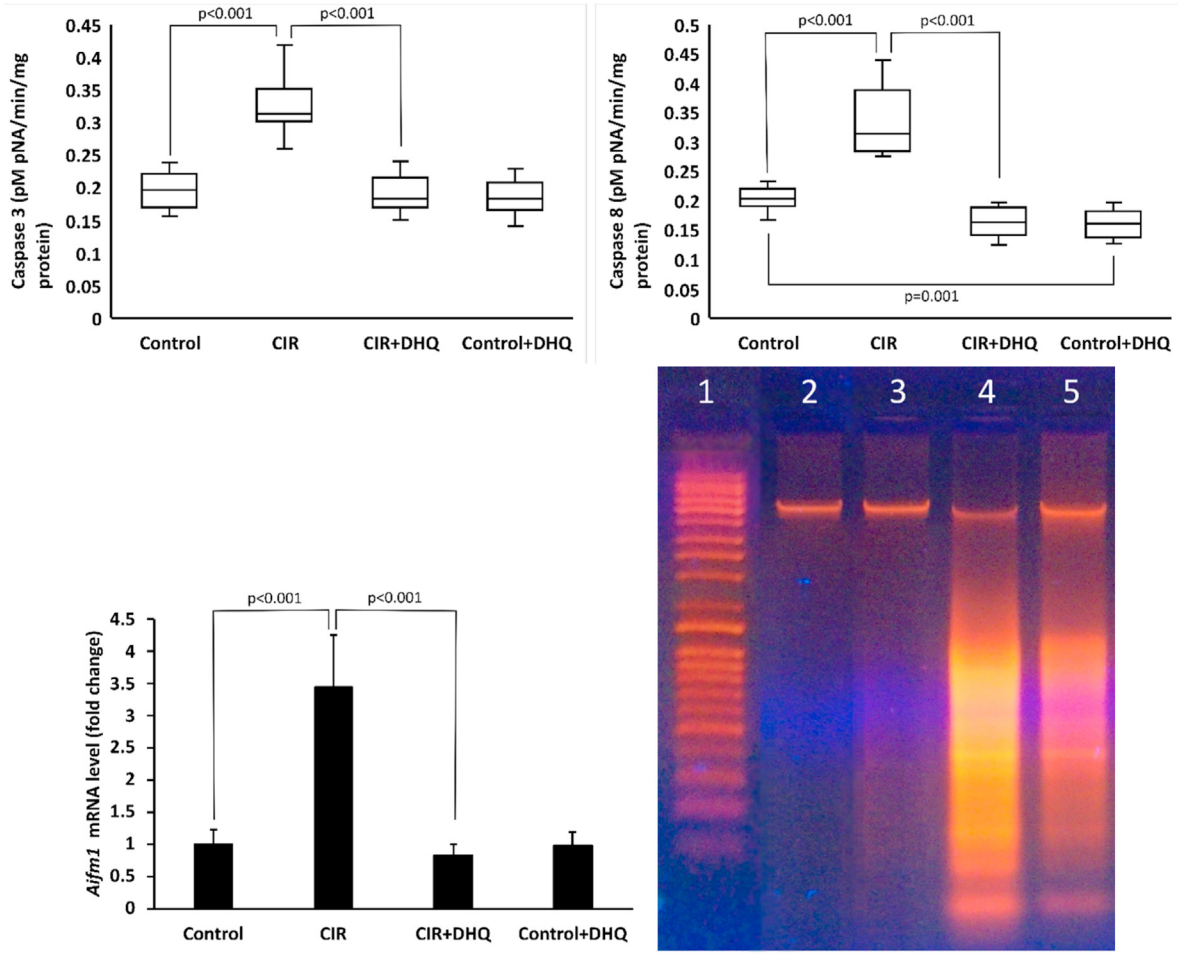

Fig. 6. The effect of DHQ on apoptotic processes in animals with CIR. DHQ promotes a decrease in the activity of caspase-3 and caspase-8, in the expression of the Aif factor and reduction of DNA fragmentation in the brain of CIR rats. The electrophoregram shows: 1 – Molecular weight markers; 2 - Control (non-degraded DNA); 3 - Control + DHQ (non-degraded DNA); 4 - CIR (apoptotic DNA ladder is visualized); 5 - CIR + DHQ (apoptotic DNA ladder is less expressed). Data in bars are presented as mean ± SD.

after a stroke and promotes the penetration of peripheral leukocytes into the damaged brain [48]. According to our data, the levels of transcripts of the proinflammatory cytokines IL-1β, IL-6, TNF-α, as well as the *Ptgs2* gene encoding the enzyme cyclooxygenase-2, were significantly increased in CIR rats. Cyclooxygenase-2 metabolizes arachidonic acid into oxidized fatty acids - prostaglandins, involved in the inflammatory response [49]. CIR stimulates the TLR4-mediated signaling pathway, followed by the rapid translocation of NF-κB from the cytoplasm into the nucleus and activation of the expression of inflammatory mediators such as IL-1, TNF-α, and IL-6, which contribute to ischemic brain damage [50]. The *Nfkb2* gene of the p100 precursor subunit of NF-κB also activates its expression [51]. In addition, our results showed that CIR was associated with an increase in MPO activity. MPO generates a wide variety of oxidants such as hypochlorous acid and nitrogen dioxide radicals [52]. DHQ, in turn, decreased MPO activity, as well as the expression of *Nfkb2* and the IL-1β, IL-6, and TNF-α cytokine genes. Apparently, these changes could be associated with the antioxidant effect of DHQ, leading to a decrease in the oxidative stress-induced inflammation.

Long-living ROS generated by CIR diffuse between organelles and between cells. They can stimulate both cell survival and pro-apoptotic signaling cascades. Oxidative damage to the endoplasmic reticulum and mitochondrial membrane causes the release of Ca^{2+} and mitochondrial proapoptotic proteins such as cytochrome *c*, Smac/DIABLO, AIF, and endonuclease G into the cytosol. Apoptosis is the dominant pathway of cell death in the ischemic penumbra. Apoptosis also leads to DNA fragmentation, degradation and cross-linking of cytoskeletal and nuclear proteins, the formation of apoptotic bodies, the expression of ligands for receptors of phagocytic cells and, finally, to microglia and astrocyte-mediated phagocytosis [53]. Key enzymes of apoptosis include the main effector caspase-3, and initiating caspases, in particular caspase-8 [54]. We have shown an increase in the activity of caspase-3, caspase-8, and DNA fragmentation in CIR rats. An increase in the expression of the proapoptotic protein AIF was also observed, which may be associated with the overexpression of Bid and Bax, forming megapores on the outer mitochondrial membrane, through which proapoptotic proteins pass into the cytosol [53,55]. CIR + DHQ rats showed reducing caspase activity, AIF expression, and DNA fragmentation. Probably, exhibiting an antioxidant effect, DHQ provided the reducing of ROS-induced apoptosis, inflammatory cytokines expression and subsequent ligand-mediated pathways of apoptosis.

Under pathophysiological conditions, antioxidant enzymes are responsible for regulating the redox balance in neurons. The functioning of some antioxidant enzymes is associated with the GSH, an oligopeptide containing a cysteine residue, cleaving unfavorable disulfide bonds of oxidized proteins. Oxidized glutathione molecules form disulfide bonds, and can be reduced back into GSH by GR. GSH can also reduce the accumulation of prooxidant xenobiotic agents through GT-catalyzed conjugation. GSH also serves as

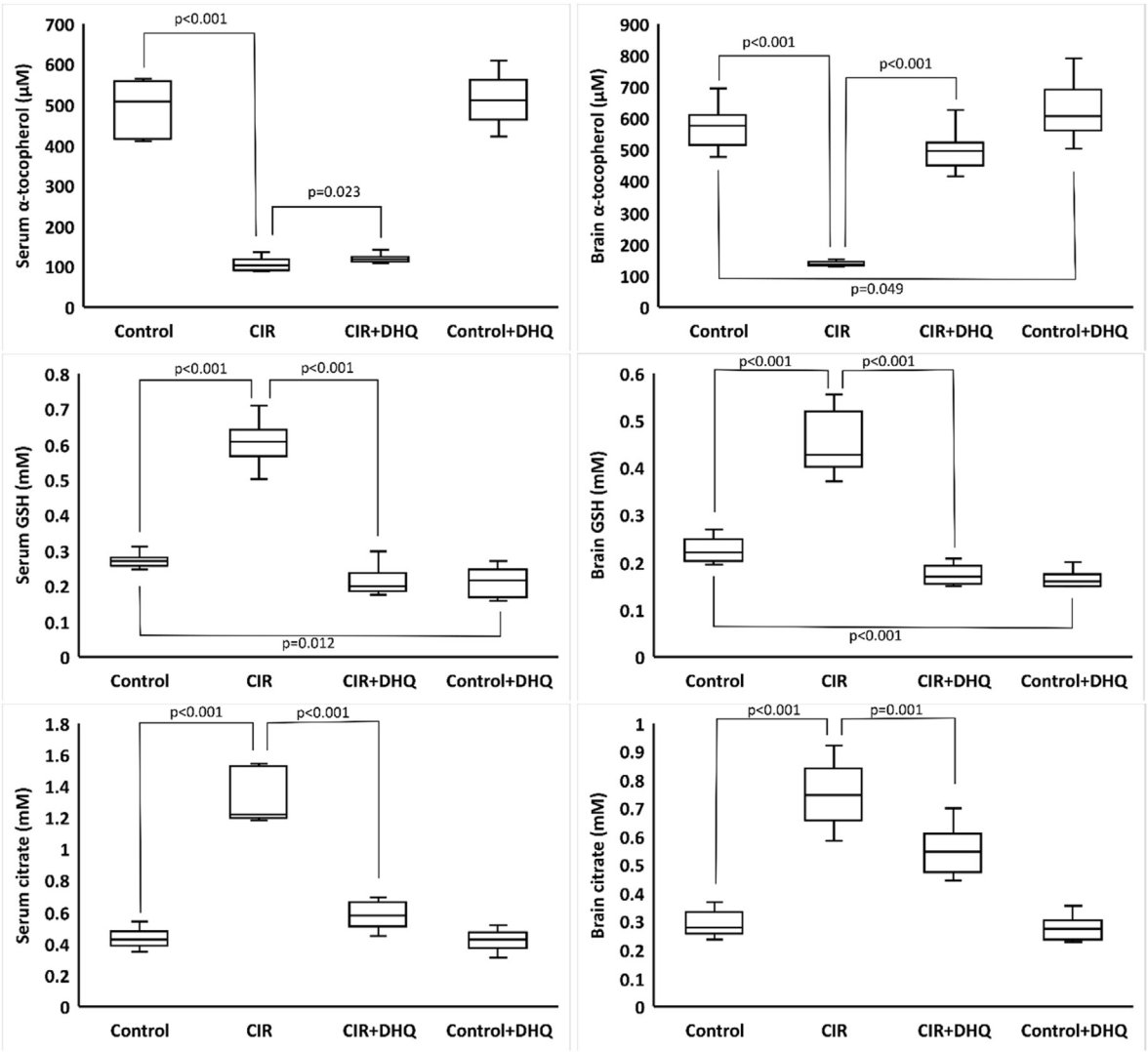

Fig. 7. Effect of DHQ on the concentration of non-enzymatic antioxidants in tissues of animals with CIR. DHQ led to a decrease in the concentration of GSH and citrate, an increase in which was associated with the development of CIR. DHQ also provided the restoration of the α-tocopherol pool in animal tissues.

a cofactor for the GP enzymes family. All GP enzymes have the ability to catalyze the degradation of organic hydroperoxides, but some isoforms are capable of reducing more complex hydroperoxides [56]. NADPH is an important metabolic product of the pentose phosphate pathway (PPP), which is used to maintain catalase stability and restore oxidized glutathione in the GR reaction. G6PDH is considered a key PPP enzyme, synthesizing NADPH and protects the brain from ischemic damage [4]. NADP-IDH is another enzyme generating NADPH, localized primarily in cytosol and mitochondria [57]. Catalase is a component of cellular peroxisomes responsible for converting hydrogen peroxide into water and molecular oxygen. Catalase is ubiquitously expressed by the neurons and glia of the central nervous system and it is one of the most efficient enzymes found in nature. Enzymes of the SOD family are responsible for the conversion of superoxide radical anions into H_2O_2. Since oxidative stress is a pathological sign of neurodegeneration, SOD dysfunction is associated with diseases characterized by neuronal loss [56]. As our data showed, animals with CIR had a significant increase in the activity of SOD, catalase, GP, GR, and GT in the brain and blood serum. These changes may indicate the development of a compensatory response to oxidative stress by the time rats were removed from the experiment. In addition, animals with the pathology were characterized by the depletion of the α-tocopherol pool. α-tocopherol is the most active antioxidant among tocopherols, protecting cells against H_2O_2-induced lipid peroxidation by enhancing antioxidant enzyme systems and reducing apoptosis caused by oxidative stress. In addition to its antioxidant properties, α-tocopherol acts as a regulator of genes involved in lipid metabolism, inflammation, and the immune system [58]. The accumulation of citrate was observed in the tissues of rats with the pathology. This finding may be associated with the inhibition of the main citrate-metabolizing enzyme - AH under oxidative stress. At the same time, citrate can also possess an antioxidant effect, due to the presence of three carboxyl groups capable of chelating metal ions in its structure [59]. The administration of DHQ to CIR rats led to a change in all analyzed parameters towards the control value. Apparently, the antioxidant effect of DHQ contributed to a decrease of oxidative stress and the mobilization of the antioxidant system decreased. Some enzymes of the antioxidant system in the CIR + DHQ group were characterized by lower values than in the control group. These differences may be associated with the development of a certain degree of oxidative stress in animals of the control group that underwent a sham operation, while the administration of DHQ inhibited oxidative stress. In addition, a decrease in the serum activity of some enzymes may indicate an improvement in the state of the BBB and a

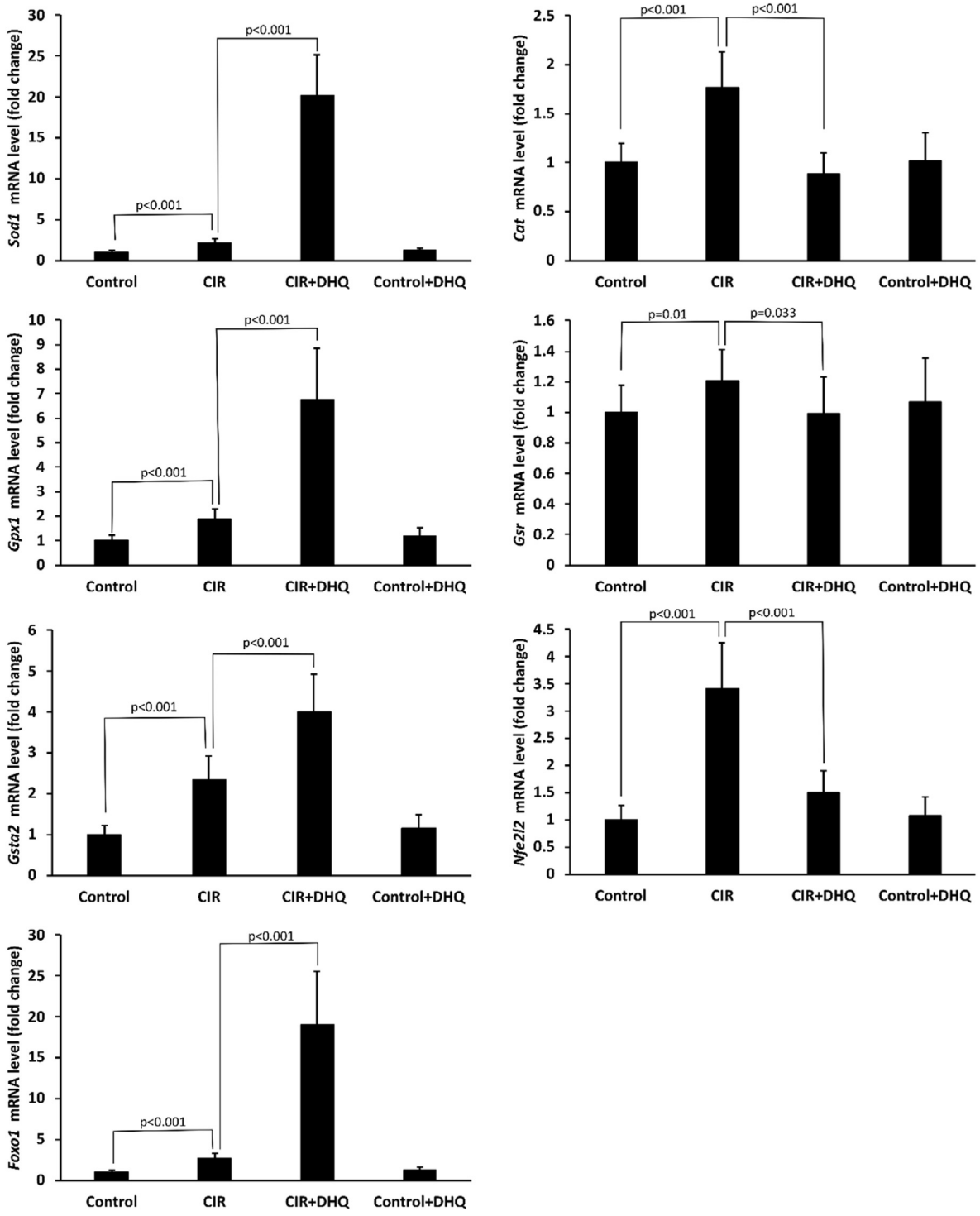

Fig. 8. The effect of DHQ on the transcriptional regulation of antioxidant defense in CIR. The heat map shows that the administration of DHQ to rats with CIR led to a decrease in the expression of *Cat*, *Gsr*, and *Nfe2l2*, as well as to an increase in the expression of *Sod1*, *Gpx1*, *Gsta2*, and *Foxo1*. Data in bars are presented as mean ± SD.

decrease in the release of enzymes from cells into the bloodstream.

The antioxidant system is able to change its functional activity under stress conditions. One of the most important mechanisms for mobilizing the activity of the antioxidant system is the transcriptional regulation of their expression. We have shown that CIR is associated with an increase in the mRNA of antioxidant enzyme genes. In addition, the expression of Nrf2 and FOXO1 transcription factors increased in pathology. Under physiological conditions, Nrf2 binds to its natural inhibitor Keap1 in the cytosol. In response to cellular damage, Nrf2 is released from Keap1, accumulates in the cytoplasm, translocates to the nucleus, heterodimerizes with bZIP proteins and recognizes the corresponding ARE sequence [60]. FOXO1 modulates numerous targets such as genes involved in apoptosis and autophagy, antioxidant enzymes, cell cycle arrest genes, and metabolic and immune regulators. Oxidative stress, mediated by the accumulation of ROS, causes a significant increase in the transcriptional activity of FOXO1, and this has a large effect on the expression of SOD and catalase. In addition, a low level of

FOXO1 can cause the decreased transcription of antioxidant enzymes in many diseases [61]. As we have shown, the administration of DHQ to CIR rats was accompanied by a decrease in the expression of catalase, GR, and Nrf2 genes. At the same time, the expression of SOD, GP, and GT genes increased. These changes may indicate that DHQ has the ability to activate some components of the antioxidant system in CIR. Such stimulation could occur through the FOXO1 factor, the mRNA level of which also increased in rats of the CIR + DHQ group. It was shown that this transcription factor increased the expression of such enzymes as SOD and GP in response to oxidative stress in β-cells of the pancreas [62]. Thus, in CIR + DHQ animals the expression of catalase, GR, and Nrf2 approached the control values at the time of withdrawal from the experiment, while the expression of SOD, GP, GT, and FOXO1 was still significantly increased as a result of the enhancement of the adaptive response by DHQ. At the same time, the mechanisms of FOXO1 regulation are extremely complex and have not yet been fully elucidated [61].

5. Conclusions

In this study, we demonstrated that DHQ has a neuroprotective effect in CIR rats, reducing histopathological changes in the brain, normalizing pyruvate and lactate levels, and decreasing HIF-1 expression. The main mechanisms of the DHQ neuroprotective action are based on its antioxidant activity, which leads to reduce oxidative stress-induced inflammation and apoptosis. In addition, the tested compound modulates the functioning and transcriptional regulation of the antioxidant system, thereby providing an additional protective effect via the regulation of the antioxidant defense in experimental animals.

Funding

This work was supported by the Council for grants of President of Russian Federation for young scientists-candidates of sciences MK-254.2020.4.

Declaration of competing interest

The authors declare that they have no known competing financial interests or personal relationships that could have appeared to influence the work reported in this paper.

Appendix 1. Synthesis of 6-hydroxy-2,2,4-trimethyl-1,2-dihydroquinoline by dealkylation of 6-ethoxy-2,2,4-trimethyl-1,2-dihydroquinoline when exposed to hydrobromic acid

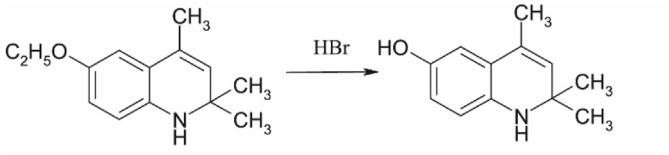

6-ethoxy-2,2,4-trimethyl-1,2-dihydroquinoline

6-hydroxy-2,2,4-trimethyl-1,2-dihydroquinoline

Appendix 2. The list of primers used in this study

Hif1a F: 5′- CATGATGGCTCCCTTTTTCA -3′ and
Hif1a R: 5′- ACATAGTAGGGGCACGGTCA -3′
Nfkb2 F: 5′- GAATTCAGCCCCTCCATTG-3′ and
Nfkb2 R: 5′- CTGAAGCCTCGCTGTTTAGG-3′
Il1b F: 5′-TGTGATGAAAGACGGCACAC -3′ and
Il1b R: 5′-CTTCTTCTTTGGGTATTGTTTGG-3′
Il6 F: 5′-CCTGGAGTTTGTGAAGAACAACT-3′ and
Il6 R: 5′-GGAAGTTGGGGTAGGAAGGA-3′
Tnf F: 5′-TCTGTGCCTCAGCCTCTTCT-3′ and
Tnf R: 5′-GGCCATGGAACTGATGAGA-3′
Ptgs2 F: 5′-TACACCAGGGCCCTTCCT-3′ and
Ptgs2 R: 5′-TCCAGAACTTCTTTTGAATCAGG-3′
Aifm1 F: 5′- AGTCCTTATTGTGGGCTTATCAAC-3′ and
Aifm1 R: 5′- TTGGTCTTCTTTAATAGTCTTGTAGGC-3′
Sod1 F: 5′-CCAGCGGATGAAGAGAGG-3′ and
Sod1 R: 5′-GGACACATTGGCCACACC-3′
Cat F: 5′-CAGCGACCAGATGAAGCA-3′ and
Cat R: 5′-GGTCAGGACATCGGGTTTC-3′
Nfe2l2 F: 5′-GCCTTGTACTTTGAAGACTGTATGC-3′ and
Nfe2l2 R: 5′-GCAAGCGACTGAAATGTAGGT-3′
Foxo1 F: 5′-AGATCTACGAGTGGATGGTGAAGAG-3′ and
Foxo1 R: 5′-GGACAGATTGTGGCGAATTGAAT-3′
Gsta2 F: 5′-CGGGAATTTGATGTTTGACC-3′ and
Gsta2 R: 5′-AGAATGGCTCTGGTCTGTGC-3′
Gpx1 F: 5′-TTTCCCGTGCAATCAGTTC-3′ and
Gpx1 R: 5′-GGACATACTTGAGGGAATTCAGA-3′
Gsr F: 5′-TTCCTCATGAGAACCAGATCC-3′ and
Gsr R: 5′-CTGAAAGAACCCATCACTGGT-3′
Gapdh F: 5′-CCCTCAAGATTGTCAGCAATG-3′ and
Gapdh R: 5′-AGTTGTCATGGATGACCTTGG-3′
Actb F: 5′- CCCGCGAGTACAACCTTCT -3′ and
Actb R: 5′- CGTCATCCATGGCGAACT -3′

Appendix 3. Prediction of the main types of biological activities of DHQ and the most promising candidates. The probability of the manifestation of biological activity ranges from zero to one

DHQ

Biological activity of the compound	Probability of activity manifestation
Reductant	0.888
Cytochrome P450 stimulant	0.870
CYP2C12 substrate	0.823
Progesterone antagonist	0.791
Chlordecone reductase inhibitor	0.790
Autoimmune disorders treatment	0.737
Kidney function stimulant	0.707
Lipid peroxidase inhibitor	0.697
Membrane integrity agonist	0.736
CYP2J substrate	0.725
Radiosensitizer	0.642
Alkane 1-monooxygenase inhibitor	0.628
CYP2J2 substrate	0.645
Glucocorticoid antagonist	0.593
Lysase inhibitor	0.616
Chemosensitizer	0.578
Menopausal disorders treatment	0.575
Free radical scavenger	0.567
Ophthalmic drug	0.565
Estrogen receptor beta antagonist	0.561
CYP2F1 substrate	0.572
MAP kinase stimulant	0.571
Anti-inflammatory	0.583

Piracetam

Biological activity of the compound	Probability of activity manifestation
Nootropic	0.876
Phobic disorders treatment	0.820
Antihypoxic	0.756
Calcium channel (voltage-sensitive) activator	0.739
Electron-transferring-flavoprotein dehydrogenase inhibitor	0.723
Anticonvulsant	0.721
Dimethylargininase inhibitor	0.725
NADPH-cytochrome-c2 reductase inhibitor	0.719
Antidyskinetic	0.714
Protein-disulfide reductase (glutathione) inhibitor	0.698
Neurotransmitter antagonist	0.681
Acetylesterase inhibitor	0.679
Fatty-acyl-CoA synthase inhibitor	0.670
Macrophage colony stimulating factor agonist	0.663
CYP2J2 substrate	0.645
UDP-glucuronosyltransferase substrate	0.612
MAP kinase stimulant	0.579
Ophthalmic drug	0.566
Estrogen receptor beta antagonist	0.561
5 Hydroxytryptamine release stimulant	0.589
Estrogen antagonist	0.552
Menopausal disorders treatment	0.556
Glucocorticoid antagonist	0.544
Glutamyl endopeptidase II inhibitor	0.592
Membrane permeability inhibitor	0.612
Glutathione thiolesterase inhibitor	0.566
Thioredoxin inhibitor	0.563
HIF1A expression inhibitor	0.554
Antiinflammatory	0.552
Free radical scavenger	0.518

SMILES code: CC1=CC(C) (C)Nc2cc(O)c(O)cc12.

Biological activity of the compound	Probability of activity manifestation
Cytochrome P450 stimulant	0.853
Reductant	0.845
Progesterone antagonist	0.798
Testosterone 17beta-dehydrogenase (NADP+) inhibitor	0.791
Autoimmune disorders treatment	0.748
CYP2J substrate	0.751
Lipid peroxidase inhibitor	0.707
CYP2C12 substrate	0.737
5 Hydroxytryptamine release stimulant	0.700
Kidney function stimulant	0.674
Radiosensitizer	0.663
Thioredoxin inhibitor	0.660
CYP2J2 substrate	0.677
Ubiquinol-cytochrome-c reductase inhibitor	0.705
Glucocorticoid antagonist	0.624
Membrane integrity agonist	0.672
Aryl-acylamidase inhibitor	0.619
Ophthalmic drug	0.599
Alkane 1-monooxygenase inhibitor	0.613
Membrane permeability inhibitor	0.644
Mucomembranous protector	0.652
Antiinflammatory	0.592
Menopausal disorders treatment	0.557
Fatty-acyl-CoA synthase inhibitor	0.573
Free radical scavenger	0.549

SMILES code: CC(=O)C1=C(N)C2=CC=CC=C2N=C1C.

Biological activity of the compound	Probability of activity manifestation
Taurine dehydrogenase inhibitor	0.839
Gluconate 2-dehydrogenase (acceptor) inhibitor	0.744
Membrane integrity agonist	0.731
Amine dehydrogenase inhibitor	0.680
Mucomembranous protector	0.667
Complement factor D inhibitor	0.602
Thiol oxidase inhibitor	0.564
Calcium channel (voltage-sensitive) activator	0.577
Endopeptidase So inhibitor	0.567
General pump inhibitor	0.574
Thioredoxin inhibitor	0.569
Leukopoiesis stimulant	0.558
Gastrin inhibitor	0.565
IgA-specific serine endopeptidase inhibitor	0.548
Oxidoreductase inhibitor	0.567
Erythropoiesis stimulant	0.543
Insulysin inhibitor	0.551
Acetylcholine neuromuscular blocking agent	0.555
Platelet aggregation stimulant	0.553
Glutamyl endopeptidase II inhibitor	0.571
Membrane permeability inhibitor	0.593
Nucleotide metabolism regulator	0.524
Aspulvinone dimethylallyltransferase inhibitor	0.593

SMILES code: CC1=CC(C) (C)Nc2c(O)cc(O)cc12.

Biological activity of the compound	Probability of activity manifestation
Reductant	0.811
Cytochrome P450 stimulant	0.796
Lipid peroxidase inhibitor	0.749
Testosterone 17beta-dehydrogenase (NADP+) inhibitor	0.766
CYP2C12 substrate	0.765
Kidney function stimulant	0.724
Progesterone antagonist	0.710
Membrane integrity agonist	0.736
CYP2J substrate	0.725
Ubiquinol-cytochrome-c reductase inhibitor	0.730
Autoimmune disorders treatment	0.676
Antiseborrheic	0.691
Antiasthmatic	0.661
Alkane 1-monooxygenase inhibitor	0.657
Radiosensitizer	0.632

(continued on next page)

SMILES code: CC(=O)\C=C\C1=CC2=C(C=C1)N(CC3=CC=CC=C3)C(C) (C)C=C2C.

Biological activity of the compound	Probability of activity manifestation
Antiarthritic	0.771
Antiallergic	0.707
Antiasthmatic	0.694
Mucomembranous protector	0.646
Antiulcerative	0.577
Reductant	0.522
Cytochrome P450 stimulant	0.502
HIF1A expression inhibitor	0.511
CYP2J substrate	0.556

Appendix 4. Effect of DHQ on the activity of antioxidant enzymes in animals with CIR. The administration of DHQ to animals with CIR led to a decrease in oxidative stress and a decrease in the activity of enzymes such as SOD, catalase, GP, GR, and GT. There was also a decrease in the activity of enzymes supplying NADPH for the functioning of the glutathione antioxidant system, NADP-IDH and G6PDH. Data are presented as mean ± SD. * - $p < 0.05$ compared to Control; ** - $p < 0.05$ compared to CIR

Groups	Blood serum				Brain			
	Control	CIR	CIR + DHQ	Control + DHQ	Control	CIR	CIR + DHQ	Control + DHQ
SOD, U/ml serum, U/g brain tissue	0.633 ± 0.15	1.367 ± 0.34*	0.560 ± 0.14**	0.557 ± 0.14*	3.43 ± 0.85	11.80 ± 2.84*	3.12 ± 0.81**	3.05 ± 0.73*
Catalase, U/ml serum, U/g brain tissue	0.109 ± 0.025	0.288 ± 0.071*	0.102 ± 0.034**	0.095 ± 0.031*	0.152 ± 0.036	0.368 ± 0.058*	0.180 ± 0.041**	0.131 ± 0.031*
GP, U/ml serum, U/g brain tissue	0.059 ± 0.014	0.111 ± 0.024*	0.095 ± 0.015**	0.052 ± 0.007	0.073 ± 0.018	0.244 ± 0.058*	0.078 ± 0.026**	0.067 ± 0.021
GR, U/ml serum, U/g brain tissue	0.023 ± 0.005	0.079 ± 0.019*	0.043 ± 0.011**	0.020 ± 0.007*	0.034 ± 0.008	0.143 ± 0.034*	0.063 ± 0.021**	0.029 ± 0.07*
GT, U/ml serum, U/g brain tissue	0.038 ± 0.009	0.086 ± 0.020*	0.047 ± 0.015**	0.032 ± 0.010*	0.082 ± 0.019	0.474 ± 0.114*	0.100 ± 0.028**	0.073 ± 0.021*
NADP-IDH, U/ml serum, U/g brain tissue	0.036 ± 0.01	0.106 ± 0.031*	0.029 ± 0.087**	0.029 ± 0.075*	0.085 ± 0.021	0.270 ± 0.057*	0.095 ± 0.031**	0.081 ± 0.024
G6PDH, U/ml serum U/g brain tissue	0.018 ± 0.004	0.049 ± 0.013*	0.010 ± 0.0025**	0.010 ± 0.0023*	0.110 ± 0.019	0.390 ± 0.092*	0.164 ± 0.042**	0.105 ± 0.021

Appendix 5. Specific activity of antioxidant enzymes in experimental animals. Data are presented as mean ± SD. * - $p < 0.05$ compared to Control; ** - $p < 0.05$ compared to CIR

Groups	Blood serum				Brain			
	Control	CIR	CIR + DHQ	Control + DHQ	Control	CIR	CIR + DHQ	Control + DHQ
SOD, U/mg protein	0.019 ± 0.004	0.041 ± 0.010*	0.015 ± 0.004**	0.015 ± 0.003*	0.103 ± 0.025	0.354 ± 0.088*	0.075 ± 0.021**	0.073 ± 0.019*
Catalase, U/mg protein	0.0039 ± 0.0010	0.0074 ± 0.0021*	0.0036 ± 0.0010**	0.0033 ± 0.0009*	0.019 ± 0.0046	0.047 ± 0.0110*	0.017 ± 0.0043**	0.015 ± 0.0041*
GP, U/mg protein	0.0015 ± 0.0003	0.0029 ± 0.0007*	0.0026 ± 0.0007**	0.0014 ± 0.0006	0.011 ± 0.003	0.021 ± 0.005*	0.018 ± 0.005**	0.009 ± 0.002*
GR, U/mg protein	0.0008 ± 0.0002	0.0022 ± 0.0005*	0.0013 ± 0.0004**	0.0006 ± 0.0002*	0.0047 ± 0.0011	0.0153 ± 0.0037*	0.0063 ± 0.0018**	0.0041 ± 0.0013*
GT, U/mg protein	0.0013 ± 0.0003	0.0027 ± 0.0006*	0.0016 ± 0.0005**	0.0011 ± 0.0003*	0.0064 ± 0.015	0.0250 ± 0.006*	0.0066 ± 0.0018**	0.0055 ± 0.0014*
NADP-IDH, U/mg protein	0.0013 ± 0.0003	0.0028 ± 0.0008*	0.0010 ± 0.0003**	0.0010 ± 0.0003*	0.011 ± 0.0028	0.024 ± 0.0054*	0.012 ± 0.0034**	0.010 ± 0.0031
G6PDH, U/mg protein	0.0010 ± 0.0002	0.0018 ± 0.0004*	0.0006 ± 0.0002**	0.0006 ± 0.0002*	0.013 ± 0.003	0.038 ± 0.007*	0.024 ± 0.0071**	0.012 ± 0.0031

References

[1] T. Peng, Y. Jiang, M. Farhan, P. Lazarovici, L. Chen, W. Zheng, Anti-inflammatory effects of traditional Chinese medicines on preclinical *in vivo* models of brain ischemia-reperfusion-injury: prospects for neuroprotective drug discovery and therapy, Front. Pharmacol. 10 (2019) 204, https://doi.org/10.3389/fphar.2019.00204.

[2] A. Kahl, A. Stepanova, C. Konrad, C. Anderson, G. Manfredi, P. Zhou, C. Iadecola, A. Galkin, Critical role of flavin and glutathione in complex I–mediated bioenergetic failure in brain ischemia/reperfusion injury, Stroke 49 (2018) 1223–1231, https://doi.org/10.1161/STROKEAHA.117.019687.

[3] T.H. Sanderson, J.M. Wider, I. Lee, C.A. Reynolds, J. Liu, B. Lepore, R. Tousignant, M.J. Bukowski, H. Johnston, A. Fite, S. Raghunayakula, J. Kamholz, L.I. Grossman, K. Przyklenk, M. Hüttemann, Inhibitory modulation of cytochrome *c* oxidase activity with specific near-infrared light wavelengths attenuates brain ischemia/reperfusion injury, Sci. Rep. 8 (2018) 3481, https://doi.org/10.1038/s41598-018-21869-x.

[4] L. Cao, D. Zhang, J. Chen, Y.Y. Qin, R. Sheng, X. Feng, Z. Chen, Y. Ding, M. Li, Z.H. Qin, G6PD plays a neuroprotective role in brain ischemia through promoting pentose phosphate pathway, Free Radic. Biol. Med. 112 (2017) 433–444, https://doi.org/10.1016/j.freeradbiomed.2017.08.011.

[5] B.A. Freeman, J.D. Crapo, Biology of disease: free radicals and tissue injury, Lab. Invest. 47 (1982) 412–426.

[6] I. Bellezza, I. Giambanco, A. Minelli, R. Donato, Nrf2-Keap1 signaling in oxidative and reductive stress, Biochim. Biophys. Acta Mol. Cell Res. 1865 (2018) 721–733, https://doi.org/10.1016/j.bbamcr.2018.02.010.

[7] H. Ren, Y. Shao, C. Wu, X. Ma, C. Lv, Q. Wang, Metformin alleviates oxidative stress and enhances autophagy in diabetic kidney disease via AMPK/SIRT1-FoxO1 pathway, Mol. Cell. Endocrinol. 500 (2020) 110628, https://doi.org/10.1016/j.mce.2019.110628.

[8] F. Carlomosti, M. D'Agostino, S. Beji, A. Torcinaro, R. Rizzi, G. Zaccagnini, B. Maimone, V. Di Stefano, F. De Santa, S. Cordisco, A. Antonini, R. Ciarapica, E. Dellambra, F. Martelli, D. Avitabile, M.C. Capogrossi, A. Magenta, Oxidative stress-induced miR-200c disrupts the regulatory loop among SIRT1, FOXO1, and eNOS, Antioxidants Redox Signal. 27 (2017) 328–344, https://doi.org/10.1089/ars.2016.6643.

[9] D.L. Bernstein, V. Zuluaga-Ramirez, S. Gajghate, N.L. Reichenbach, B. Polyak, Y. Persidsky, S. Rom, miR-98 reduces endothelial dysfunction by protecting blood–brain barrier (BBB) and improves neurological outcomes in mouse ischemia/reperfusion stroke model, J. Cerebr. Blood Flow Metabol. 40 (2020) 1953–1965, https://doi.org/10.1177/0271678X19882264.

[10] X. Liu, X. Zhang, F. Wang, X. Liang, Z. Zeng, J. Zhao, H. Zheng, X. Jiang, Y. Zhang, Improvement in cerebral ischemia–reperfusion injury through the TLR4/NF-κB pathway after Kudiezi injection in rats, Life Sci. 191 (2017) 132–140, https://doi.org/10.1016/j.lfs.2017.10.035.

[11] L. Gong, Y. Tang, R. An, M. Lin, L. Chen, J. Du, RTN1-C mediates cerebral ischemia/reperfusion injury via ER stress and mitochondria-associated apoptosis pathways, Cell Death Dis. 8 (2017), e3080, https://doi.org/10.1038/cddis.2017.465.

[12] S. Merel, J. Regueiro, M.H.G. Berntssen, R. Hannisdal, R. Ørnsrud, N. Negreira, Identification of ethoxyquin and its transformation products in salmon after controlled dietary exposure via fish feed, Food Chem. 289 (2019) 259–268, https://doi.org/10.1016/j.foodchem.2019.03.054.
[13] YuA. Ivanov, N.L. Zaichenko, S.V. Rykov, O.Ya Grinberg, A.A. Dubinsky, S.D. Pirozhkov, E.G. Rozantsev, I.E. Pokrovskaya, A.B. Shapiro, Synthesis of oxy-, acyl-, oxo-, N-oxides of oxo- and morpholillox- derived hydrogenated quinolines and study of their radical analogues by EPR, Izv, USSR Acad. Sci. Ser. chem. 8 (1979) 1800–1807.
[14] PASS Online. http://www.pharmaexpert.ru/passonline/index.php (accessed 28 February 2021).
[15] S.O. Rotimi, O.A. Rotimi, I.B. Adelani, C. Onuzulu, P. Obi, R. Okungbaye, Stevioside modulates oxidative damage in the liver and kidney of high fat/low streptozocin diabetic rats, Heliyon 4 (2018), e00640, https://doi.org/10.1016/j.heliyon.2018.e00640.
[16] S.T. Shah, W.A. Yehya, O. Saad, K. Simarani, Z. Chowdhury, A.A. Alhadi, L.A. Al-Ani, Surface Functionalization of Iron Oxide Nanoparticles with Gallic Acid as Potential Antioxidant and Antimicrobial Agents, 7, 2017, p. 306, https://doi.org/10.3390/nano7100306.
[17] M. Roman, D.L. Roman, V. Ostafe, A. Ciorsac, A. Isvoran, Computational assessment of pharmacokinetics and biological effects of some anabolic and androgen steroids, Pharmaceut. Res. 35 (2018) 41, https://doi.org/10.1007/s11095-018-2353-1.
[18] ProTox-II - prediction of toxicity of Chemicals. http://tox.charite.de/protox_II/index.php?site=home (accessed 30 January 2020).
[19] S. Chacko, S. Samanta, A novel approach towards design, synthesis and evaluation of some Schiff base analogues of 2-aminopyridine and 2-aminobezothiazole against hepatocellular carcinoma, Biomed. Pharmacother. 89 (2017) 162–176, https://doi.org/10.1016/j.biopha.2017.01.108.
[20] L. Mendes, S. Angélica, P. Schiavon, H. Milani, R. Maria, W. Oliveira, Cognitive impairment and persistent anxiety-related responses following bilateral common carotid artery occlusion in mice, Behav. Brain Res. 249 (2013) 28–37, https://doi.org/10.1016/j.bbr.2013.04.010.
[21] I.M. Piskarev, S.V. Trofimova, I.P. Ivanova, O.E. Burkhina, Investigation of the level of free-radical processes in substrates and biological samples using induced chemiluminescence, Biophysics 60 (2015) 400–408, https://doi.org/10.1134/S0006350915030148.
[22] A.Z. Reznick, L. Packer, Oxidative damage to proteins: spectrophotometric method for carbonyl assay, Methods Enzymol. 233 (1994) 357–363, https://doi.org/10.1016/S0076-6879(94)33041-7.
[23] R.O. Recknagel, A.K. Ghoshal, Lipoperoxidation of rat liver microsomal lipids induced by carbon tetrachloride, Nature 210 (1966) 1162–1163, https://doi.org/10.1038/2101162a0.
[24] K. Suzuki, H. Ota, S. Sasagawa, T. Sakatani, T. Fujikura, Assay method for myeloperoxidase in human polymorphonuclear leukocytes, Anal. Biochem. 132 (1983) 345–352, https://doi.org/10.1016/0003-2697(83)90019-2.
[25] M. Nishikimi, N.A. Rao, K. Yagi, The occurrence of superoxide anion in the reaction of reduced phenazine methosulphate and molecular oxygen, Biochem. Biophys. Res. Co 46 (1972) 849–864, https://doi.org/10.1016/s0006-291x(72)80218-3.
[26] L. Góth, A simple method for determination of serum catalase activity and revision of reference range, Clin. Chim. Acta 196 (1991) 143–151, https://doi.org/10.1016/0009-8981(91)90067-m.
[27] D.E. Paglia, W.N. Valentine, Studies on the quantitative and qualitative characterization of erythrocyte glutathione peroxidase, Lab. Clin. Med. 70 (1967) 158–169.
[28] G. Zanetti, Rabbit liver glutathione reductase. Purification and properties, Arch. Biochem. Biophys. 198 (1979) 241–246, https://doi.org/10.1016/0003-9861(79)90415-6.
[29] M. Warholm, C. Guthenberg, C. Von Bahr, B. Mannervik, Glutathione transferases from human liver, Methods Enzymol. 113 (1985) 499–504, https://doi.org/10.1016/s0076-6879(85)13065-x.
[30] G.L. Ellman, Tissue sulfhydryl groups, Arch. Biochem. Biophys. 82 (1959) 70–77, https://doi.org/10.1016/0003-9861(59)90090-6.
[31] J.M. Valdez, A.F.M. Johnstone, J.E. Richards, J.E. Schmid, J.E. Royland, P.R.S. Kodavanti, Interaction of diet and ozone exposure on oxidative stress parameters within specific brain regions of male brown Norway rats, Int. J. Mol. Sci. 20 (2018) 11, https://doi.org/10.3390/ijms20010011.
[32] I.D. Desai, F.E. Martinez, Bilirubin interference in the colorimetric assay of plasma vitamin E, Clin. Chim. Acta 154 (1986) 247–250, https://doi.org/10.1016/0009-8981(86)90040-9.
[33] The department of organic Chemistry of Voronezh state University. http://www.chem.vsu.ru/files/upload/files/vgu_scrining.db, accessed: 11 April 2021.
[34] E.D. Kryl'skii, T.N. Popova, O.A. Safonova, A.O. Stolyarova, G.A. Razuvaev, M.A. Pinheiro de Carvalho, Transcriptional regulation of antioxidant enzymes activity and modulation of oxidative stress by melatonin in rats under cerebral ischemia/reperfusion conditions, Neuroscience 406 (2019) 653–666, https://doi.org/10.1016/j.neuroscience.2019.01.046.
[35] A.V. Makeeva, T.N. Popova, Effects of thioctic acid on the glutathione redox cycle after cerebral ischemia-reperfusion in rats, Neurochem. J. 3 (2009) 110–117, https://doi.org/10.1134/S1819712409020068.
[36] A.V. Makeeva, T.N. Popova, O.V. Sukhoveeva, L.F. Panchenko, Effects of guanidine derivatives on the activities of superoxide dismutase and catalase during postischemic reperfusion in the rat brain, Neurochem. J. 4 (2010) 217–221, https://doi.org/10.1134/S1819712410030098.
[37] J. Zhang, Z. Deng, J. Liao, C. Song, C. Liang, H. Xue, L. Wang, K. Zhang, G. Yan, Leptin attenuates cerebral ischemia injury through the promotion of energy metabolism via the PI_3K/Akt pathway, J. Cerebr. Blood Flow Metabol. 33 (2013) 567–574, https://doi.org/10.1038/jcbfm.2012.202.
[38] O. Vetrovoy, E. Rybnikova, Neuroprotective action of PHD inhibitors is predominantly HIF-1-independent, J. Neurochem. 150 (2019) 645–647, https://doi.org/10.1111/jnc.14822.
[39] S. Page, S. Raut, A. Al-Ahmad, Oxygen-glucose deprivation/reoxygenation-induced barrier disruption at the human blood–brain barrier is partially mediated through the HIF-1 pathway, NeuroMolecular Med. 21 (2019) 414–431, https://doi.org/10.1007/s12017-019-08531-z.
[40] M. Xia, Q. Ding, Z. Zhang, Q. Feng, Remote limb ischemic preconditioning protects rats against cerebral ischemia via HIF-1α/AMPK/HSP70 pathway, Cell. Mol. Neurobiol. 37 (2017) 1105–1114, https://doi.org/10.1007/s10571-016-0444-2.
[41] A. Kanavaki, K. Spengos, M. Moraki, P. Delaporta, C. Kariyannis, I. Papassotiriou, A. Kattamis, Serum levels of S100b and NSE proteins in patients with non-transfusion-dependent thalassemia as biomarkers of brain ischemia and cerebral vasculopathy, Int. J. Mol. Sci. 18 (2017) 2724, https://doi.org/10.3390/ijms18122724.
[42] Z. Lou, A.P. Wang, X.M. Duan, G.H. Hu, G.L. Song, M.L. Zuo, Z.B. Yang, Upregulation of NOX2 and NOX4 mediated by TGF-β signaling pathway exacerbates cerebral ischemia/reperfusion oxidative stress injury, Cell. Physiol. Biochem. 46 (2018) 2103–2113, https://doi.org/10.1159/000489450.
[43] L. Wu, X. Xiong, X. Wu, Y. Ye, Z. Jian, Z. Zhi, Li Gu, Targeting oxidative stress and inflammation to prevent ischemia-reperfusion injury, Front. Mol. Neurosci. 13 (2020) 28, https://doi.org/10.3389/fnmol.2020.00028.
[44] A. Janyou, P. Wicha, J. Jittiwat, A. Suksamrarn, C. Tocharus, J. Tocharus, Dihydrocapsaicin attenuates blood brain barrier and cerebral damage in focal cerebral ischemia/reperfusion via oxidative stress and inflammatory, Sci. Rep. 7 (2017) 10556, https://doi.org/10.1038/s41598-017-11181-5.
[45] M. Gu, M.M. Iravani, J.M. Cooper, D. King, P. Jenner, A.H. Schapira, Pramipexole protects against apoptotic cell death by non-dopaminergic mechanisms, J. Neurochem. 91 (2004) 1075–1081, https://doi.org/10.1111/j.1471-4159.2004.02804.x.
[46] J. Zhu, V.A. Carozzi, N. Reed, R. Mi, P. Marmiroli, G. Cavaletti, A. Hoke, Ethoxyquin provides neuroprotection against cisplatin-induced neurotoxicity, Sci. Rep. 6 (2016) 28861, https://doi.org/10.1038/srep28861.
[47] M.I. Fernández-Bachiller, C. Pérez, G.C. González-Muñoz, S. Conde, M.G. López, M. Villarroya, A.G. García, M.I. Rodríguez-Franco, Novel tacrine–8-hydroxyquinoline hybrids as multifunctional agents for the treatment of Alzheimer's disease, with neuroprotective, cholinergic, antioxidant, and copper-complexing properties, J. Med. Chem. 53 (2010) 4927–4937, https://doi.org/10.1021/jm100329q.
[48] K. Shi, D.C. Tian, Z.G. Li, A.F. Ducruet, M.T. Lawton, F.D. Shi, Global brain inflammation in stroke, Lancet Neurol. 18 (2019) 1058–1066, https://doi.org/10.1016/S1474-4422(19)30078-X.
[49] D.E. López, S.J. Ballaz, The role of brain cyclooxygenase-2 (Cox-2) beyond neuroinflammation: neuronal homeostasis in memory and anxiety, Mol. Neurobiol. 57 (2020) 5167–5176, https://doi.org/10.1007/s12035-020-02087-x.
[50] X. Li, L. Su, X. Zhang, C. Zhang, L. Wang, Y. Li, Y. Zhang, T. He, X. Zhu, L. Cui, Ulinastatin downregulates TLR4 and NF-kB expression and protects mouse brains against ischemia/reperfusion injury, Neurol. Res. 39 (2017) 367–373, https://doi.org/10.1080/01616412.2017.1286541.
[51] H.Y. Wei, X. Ma, Tamoxifen reduces infiltration of inflammatory cells, apoptosis and inhibits the IKK/NF-kB pathway after spinal cord injury in rats, Neurol. Sci. 35 (2014) 1763–1768, https://doi.org/10.1007/s10072-014-1828-z.
[52] G. Yu, Y. Liang, S. Zheng, H. Zhang, Inhibition of myeloperoxidase by N-acetyl lysyltyrosylcysteine amide reduces oxidative stress–mediated inflammation, neuronal damage, and neural stem cell injury in a murine model of stroke, J. Pharmacol. Exp. Therapeut. 364 (2018) 311–322, https://doi.org/10.1124/jpet.117.245688.
[53] A.B. Uzdensky, Apoptosis regulation in the penumbra after ischemic stroke: expression of pro- and antiapoptotic proteins, Apoptosis 24 (2019) 687–702, https://doi.org/10.1007/s10495-019-01556-6.
[54] F. Yin, H. Zhou, Y. Fang, C. Li, Y. He, L. Yu, H. Wan, J. Yang, Astragaloside IV alleviates ischemia reperfusion-induced apoptosis by inhibiting the activation of key factors in death receptor pathway and mitochondrial pathway, J. Ethnopharmacol. 248 (2020) 112319, https://doi.org/10.1016/j.jep.2019.112319.
[55] D. Coimbra-Costa, N. Alva, M. Duran, T. Carbonell, R. Rama, Oxidative stress and apoptosis after acute respiratory hypoxia and reoxygenation in rat brain, Redox Biol. 12 (2017) 216–225, https://doi.org/10.1016/j.redox.2017.02.014.
[56] S.M. Davis, K.R. Pennypacker, Targeting antioxidant enzyme expression as a therapeutic strategy for ischemic stroke, Neurochem. Int. 107 (2017) 23–32, https://doi.org/10.1016/j.neuint.2016.12.007.
[57] H.J. Cho, H.Y. Cho, J.W. Park, O.S. Kwon, H.S. Lee, T.L. Huh, B.S. Kang, $NADP^+$-dependent cytosolic isocitrate dehydrogenase provides NADPH in the presence of cadmium due to the moderate chelating effect of glutathione, JBIC J. Biol. Inorgan. Chem. 23 (2018) 849–860, https://doi.org/10.1007/s00775-018-1581-5.
[58] M. Wallerta, M. Zieglera, X. Wang, A. Maluenda, X. Xu, M.L. Yap, R. Witte, C. Giles, S. Kluge, M. Hortmann, J. Zhang, P. Meikle, S. Lorkowski, K. Peter, α-

Tocopherol preserves cardiac function by reducing oxidative stress and inflammation in ischemia/reperfusion injury, Redox Biol. 26 (2019) 101292, https://doi.org/10.1016/j.redox.2019.101292.
[59] X. Wu, H. Dai, L. Liu, C. Xu, Y. Yin, J. Yi, M.D. Bielec, Y. Hana, S. Li, Citrate reduced oxidative damage in stem cells by regulating cellular redox signaling pathways and represent a potential treatment for oxidative stress-induced diseases, Redox Biol. 21 (2019) 101057, https://doi.org/10.1016/j.redox.2018.11.015.
[60] R. Zhang, M. Xu, Y. Wang, F. Xie, G. Zhang, X. Qin, Nrf2—a promising therapeutic target for defensing against oxidative stress in stroke, Mol. Neurobiol. 54 (2017) 6006–6017, https://doi.org/10.1007/s12035-016-0111-0.
[61] Y. Xing, A. Li, Y. Yang, X. Li, L. Zhang, H. Guo, The regulation of FOXO1 and its role in disease progression, Life Sci. 193 (2018) 124–131, https://doi.org/10.1016/j.lfs.2017.11.030.
[62] T. Zhang, D.H. Kim, X. Xiao, S. Lee, Z. Gong, R. Muzumdar, V. Calabuig-Navarro, J. Yamauchi, H. Harashima, R. Wang, R. Bottino, J.C. Alvarez-Perez, A. Garcia-Ocaña, G. Gittes, H.H. Dong, FoxO1 plays an important role in regulating β-cell compensation for insulin resistance in male mice, Endocrinology 157 (2016) 1055–1070, https://doi.org/10.1210/en.2015-1852.